Atmospheric
Chemistry
and Physics
Discussions

1 **Biogenic and anthropogenic sources of isoprene and monoterpenes and their secondary organic**
2 **aerosol in Delhi, India**

3 Daniel J. Bryant[1], Beth S. Nelson[1], Stefan J. Swift[1a], Sri Hapsari Budisulistiorini[1], Will S. Drysdale[1,2],
4 Adam R. Vaughan[1], Mike J. Newland[1b], James R. Hopkins[1,2], James M. Cash[3,4], Ben Langford[3], Eiko
5 Nemitz[3], W. Joe F. Acton[5c], C. Nicholas Hewitt[5], Tuhin Mandal[6], Bhola R. Gurjar[6], Shivani[6d], Ranu
6 Gadi[6], James D. Lee[1,2], Andrew R. Rickard[1,2], Jacqueline F. Hamilton[1]

7 1- Wolfson Atmospheric Chemistry Laboratories, Department of Chemistry, University of York,
8 Heslington, York, YO10 5DD, UK

9 2- National Centre for Atmospheric Science, University of York, Heslington, York, YO10 5DD, UK

10 3- UK Centre for Ecology and Hydrology, Penicuik, Midlothian, Edinburgh, EH26 0QB, UK

11 4- School of Chemistry, University of Edinburgh, Edinburgh, EH9 3FJ, Edinburgh, UK

12 5- Lancaster Environment Centre, Lancaster University, Lancaster, LA1 4YW, UK

13 6- Department of Applied Sciences and Humanities, Indira Gandhi Delhi Technical University for
14 Women, Delhi, 110006, India

15 [a] now at: J. Heyrovsky Institute of Physical Chemistry, Department of Chemistry of Ions in Gaseous
16 Phase, Prague, Czech Republic

17 [b] now at: ICARE-CNRS, 1 C Av. de la Recherche Scientifique, 45071 Orléans CEDEX 2, France

18 [c] now at: School of Geography, Earth and Environmental Sciences, University of Birmingham,
19 Birmingham, B15 2TT, UK

20 [d] now at: Department of Chemistry, Miranda House, Delhi University, Delhi, 110007, India

21 Correspondence email: daniel.bryant@york.ac.uk

22 **Abstract**

23 Isoprene and monoterpenes emissions to the atmosphere are generally dominated by biogenic
24 sources. The oxidation of these compounds can lead to the production of secondary organic aerosol,
25 however the impact of this chemistry in polluted urban settings has been poorly studied. Isoprene
26 and monoterpenes can form SOA heterogeneously via anthropogenic-biogenic interactions resulting
27 in the formation of organosulfates (OS) and nitrooxy-organosulfates (NOS). Delhi, India is one of the
28 most polluted cities in the world, but little is known about the emissions of biogenic VOCs or the
29 sources of SOA. As part of the DELHI-FLUX project, gas phase mixing ratios of isoprene and speciated
30 monoterpenes were measured during pre- and post-monsoon measurement campaigns in central
31 Delhi. Nocturnal mixing ratios of the VOCs were substantially higher during the post-monsoon
32 (isoprene: (0.65 ± 0.43) ppbv, limonene: (0.59 ± 0.11) ppbv, α-pinene: (0.13 ± 0.12) ppbv) than the
33 pre-monsoon (isoprene: (0.13 ± 0.18) ppbv, limonene: 0.011 ± 0.025 (ppbv), α-pinene: 0.033 ±
34 0.009) period. At night, isoprene and monoterpene concentrations correlated strongly with CO
35 across during the post-monsoon period. This is one of the first observations in Asia, suggesting
36 monoterpene emissions are dominated by anthropogenic sources. Filter samples of particulate
37 matter less than 2.5 microns in diameter (PM$_{2.5}$) were collected and the OS and NOS content
38 analysed using ultrahigh-performance liquid chromatography tandem mass spectrometry (UHPLC-
39 MS^2). Inorganic sulfate was shown to facilitate the formation of isoprene OS species across both
40 campaigns. Sulfate contained within OS and NOS species were shown to contribute significantly to

41 the sulfate signal measured via AMS. Strong nocturnal enhancements of NOS species were observed
42 across both campaigns. The total concentration of OS/NOS species contributed an average of (2.0 ±
43 0.9) % and (1.8 ± 1.4) % to the total oxidised organic aerosol, and up to a maximum of 4.2 % and 6.6
44 % across the pre- and post-monsoon periods, respectively. Overall, this study provides the first
45 molecular level measurements of SOA derived from isoprene and monoterpene in Delhi and
46 demonstrates that both biogenic and anthropogenic sources of these compounds can be important
47 in urban areas.

48 **1. Introduction**

49 India is undergoing significant urbanization and industrialisation, with a rapidly increasing
50 population. According to the WHO, India was home to 9 out of the top 10 most polluted cities in the
51 world in 2020 in terms of annual mean $PM_{2.5}$ (particulate matter less than 2.5 micrometres in
52 diameter) concentrations (WHO, 2018). In Delhi, the population-weighted mean $PM_{2.5}$ was estimated
53 to be 209 (range: 120 – 339.5) $\mu g\ m^{-3}$ in 2017, over 40 times the WHO annual mean guidelines of 5
54 $\mu g\ m^{-3}$, and greater than five times India's own standard of 40 $\mu g\ m^{-3}$ (Balakrishnan et al., 2019). Air
55 pollution is estimated to cause over 1 million deaths per year in India alone (Landrigan et al., 2018).

56 Numerous studies have investigated $PM_{2.5}$ concentrations, characteristics and meteorological effects
57 in Delhi (Anand et al., 2019; Bhandari et al., 2020; Chowdhury et al., 2004; Hama et al., 2020;
58 Kanawade et al., 2020; Miyazaki et al., 2009; Nagar et al., 2017). The key sources of $PM_{2.5}$ identified
59 are secondary aerosol, fossil fuel combustion, municipal waste and biomass burning (Chowdhury et
60 al., 2004; Sharma and Mandal, 2017; Stewart et al., 2021b, 2021a). Previous studies have also shown
61 that alongside extremely high emissions of pollutants, regional sources and meteorology in
62 particular play an important role in high pollution events in Delhi (Bhandari et al., 2020; Sawlani et
63 al., 2019; Schnell et al., 2018; Sinha et al., 2014).

64 Secondary species have been shown to be significant contributors to PM_1 and $PM_{2.5}$ mass in Delhi,
65 with organics contributing 40-70 % of PM_1 mass. (Gani et al., 2019; Shivani et al., 2019; Reyes-
66 Villegas et al., 2021; Sharma and Mandal, 2017) However, limited molecular level analysis of organic
67 aerosol (OA) has been undertaken (Chowdhury et al., 2004; Elzein et al., 2020; Miyazaki et al., 2009;
68 Singh et al., 2021, 2012; Yadav et al., 2021). Kirillova et al., (2014) analysed the sources of water-
69 soluble organic carbon (WSOC) in Delhi, using radiocarbon measurement constraints. The study
70 identified that 79 % of WSOC was classified as non-fossil carbon, attributed to biogenic/biomass
71 burning sources in urban Delhi (Kirillova et al., 2014), similar to other studies from India (Kirillova et
72 al., 2013; Sheesley et al., 2012). Studies across Asia, Europe and North America have also shown high
73 contributions from non-fossil sources to ambient PM concentrations in urban environments (Du et
74 al., 2014; Kirillova et al., 2010; Szidat et al., 2004; Wozniak et al., 2012). The sources of this modern
75 carbon in urban areas are poorly understood, although biomass burning is a key component (Elser et
76 al., 2016; Hu et al., 2016; Lanz et al., 2010; Nagar et al., 2017). Recently in Delhi, solid-fuel
77 combustion sources such as cow dung cake or municipal solid waste have been shown to release
78 over 1000 different organic components into the aerosol phase at emission (Stewart et al., 2021a).
79 Alongside biomass burning, one potential source of this non-fossil aerosol is biogenic secondary
80 organic aerosol (BSOA), which is formed via the oxidation of biogenic volatile organic compounds
81 (BVOCs) and subsequent gas-particle phase transfer (Hallquist et al., 2009; Hoffmann et al., 1997).

82 Isoprene is the most abundant BVOC, with annual global emissions estimates of between 350 - 800
83 Tg yr^{-1} (Guenther et al., 2012; Sindelarova et al., 2014). Globally, isoprene is predominately emitted
84 from biogenic sources, but anthropogenic sources become increasingly important in urban areas
85 especially at night (Borbon et al., 2001; Hsieh et al., 2017; Khan et al., 2018a; Mishra and Sinha,

86   2020; Sahu et al., 2017; Sahu and Saxena, 2015). Monoterpenes are another important BSOA
87   precursor, with annual global emissions estimates of between 89 and 177 Tg yr^{-1} (Guenther et al.,
88   2012; Sindelarova et al., 2014). Monoterpenes while mainly biogenic, are also emitted from
89   anthropogenic sources such as biomass burning, cooking and fragranced consumer products (Cheng
90   et al., 2018; Gkatzelis et al., 2021; Panopoulou et al., 2020, 2021; Stewart et al., 2021b, 2021c; Zhang
91   et al., 2020).

92   Numerous studies have identified and quantified molecular level markers from isoprene and
93   monoterpenes, especially in the Southeastern-US and China (Brüggemann et al., 2019; Bryant et al.,
94   2020, 2021; Hettiyadura et al., 2019; Huang et al., 2016; Rattanavaraha et al., 2016b; Wang et al.,
95   2016, 2018a; Yee et al., 2020). The complex sources of isoprene and monoterpenes in highly
96   polluted urban areas make source identification difficult. As such, the SOA markers in this study will
97   be referred to as originating from isoprene or monoterpenes, but the emissions are likely from a
98   mixture of biogenic and anthropogenic sources as discussed previously. (Cash et al., 2021b; Nelson
99   et al., 2021)

100   Recent studies have started to focus on anthropogenic-biogenic interactions, whereby
101   anthropogenic pollutants such as NO_x and sulfate enhance the formation of biogenically derived SOA
102   species. Increased NO or NO_2 concentrations can lead to higher organonitrate (ON) or nitrooxy-
103   organosulfate (NOS) concentrations through RO_2 + NO or VOC + NO_3 pathways.(Morales et al., 2021;
104   Takeuchi and Ng, 2019) Inorganic sulfate formed from the oxidation of SO_2 plays a pivotal role in OS
105   and NOS formation (Bryant et al., 2020; Budisulistiorini et al., 2015; Glasius et al., 2018; Hettiyadura
106   et al., 2019; Hoyle et al., 2011; Xu et al., 2015). Sulfate allows the acid-catalysed uptake of gas phase
107   oxidation products into the particle phase. Both chamber and ambient studies have shown the direct
108   link between sulfate and OS concentrations (Brüggemann et al., 2020a; Bryant et al., 2020;
109   Budisulistiorini et al., 2015; Gaston et al., 2014; Lin et al., 2012; Riva et al., 2019; Surratt et al.,
110   2008a; Xu et al., 2015). Yee et al., (2020) highlighted markers from both the high/low-NO isoprene
111   oxidation pathways correlated linearly with sulfate over a large range of sulfate concentrations (0.01
112   – 10 µg m^{-3}) across central Amazonia during the wet and dry seasons and in the SE-US summer. They
113   conclude that the majority of isoprene oxidation products in pre-industrial settings are still expected
114   to be in the form of isoprene OS (OSi), suggesting that they cannot be thought of as purely a
115   biogenic-anthropogenic product (Yee et al., 2020).

116   In this study, offline $PM_{2.5}$ filter samples were collected across two campaigns (pre and post-
117   monsoon) in central Delhi, alongside a comprehensive suite of gas and aerosol atmospheric
118   pollutant measurements. Filters were analysed using ultra-high performance liquid chromatography
119   tandem mass spectrometry and isoprene and monoterpene OS/NOS markers identified and
120   quantified. Isoprene and monoterpene emissions were observed to correlate strongly to
121   anthropogenic markers, suggesting a mixed anthropogenic/biogenic sources of these VOCs. OSi
122   species showed strong seasonality and strong correlations to particulate sulfate. NOS species
123   showed strong nocturnal enhancements, likely due to nitrate radical chemistry. This study is the first
124   molecular level particle phase analysis of OS and NOS markers from isoprene and monoterpenes in
125   Delhi and aims to improve our understanding of the sources of isoprene and monoterpene SOA
126   markers and their formation pathways in extremely polluted urban environments.

127   **2.Experimental**

128   **2.1 Filter collection and site information**

129   PM$_{2.5}$ filter samples were collected as part of the Air Pollution and Human Health (APHH)-India
130   campaign, at the Indira Gandhi Delhi Technical University for Women in New Delhi, India, (28°39'55"
131   N 77°13'56" E). The site is situated inside the third ring road which caters to huge volumes of traffic,
132   with a major road to the east, between the site and the Yamuna River. Two train stations are located
133   to the south and southwest of the site, and there are several green spaces locally in all
134   directions.(Nelson et al., 2021; Stewart et al., 2021c) Filters were collected during two field
135   campaigns in 2018. The first campaign was during the pre-monsoon period, with 35 filters were
136   collected between 28/05/2018 and 05/06/2018. The second campaign during the post-monsoon
137   period, 108 filters were collected between 09/10/2018 and 6/11/2018. Quartz filters (Whatman
138   QMA, 10" by 8") were pre-baked at 550 °C for 5 hours and wrapped in foil before use. Samples were
139   collected using an HiVol sampler (Ecotech 3000, Victoria Australia) with selective PM$_{2.5}$ inlet at a flow
140   rate of 1.33 m^3 min^{-1}. Once collected, filters were stored in foil at -20 °C before, during and after
141   transport for UK based analysis.

2.2 Filter extraction

143   Using a standard square filter cutter, a section of filter was taken with an area of 30.25 cm^2 which
144   was then cut into roughly 1 cm^2 pieces and placed in a 20 mL glass vial. Next, 8 mL of LC-MS grade
145   methanol (MeOH, Optima, Fisher Chemical, USA) was added to the sample and sonicated for 45 min.
146   Ice packs were used to keep the bath temperature below room temperature, with the water
147   swapped mid-way through. Using a 5 mL plastic syringe, the MeOH extract was then pushed through
148   a 0.22 µm filter (Millipore) into another sample vial. An additional 2 mL (2 x 1 mL) of MeOH was
149   added to the filter sample, and then extracted through the filter to give a combined extract ~ 10mL.
150   This extract was then reduced to dryness using a Genevac solvent evaporator under vacuum. The dry
151   sample was then reconstituted in 50:50 MeOH:H$_2$O (Optima, Fisher Chemical, USA) for analysis
152   (Bryant et al., 2020; Spolnik et al., 2018). Extraction efficiencies of 2-methyl-glyceric acid (2-MG-OS)
153   and camphorsulfonic acid were determined using authentic standards spiked onto a pre-baked clean
154   filter and recoveries were calculated to be 71 % and 99 % respectively.

2.3 Ultra-high performance liquid chromatography tandem mass spectrometry (UHPLC-MS^2)

156   The extracted fractions of the filter samples were analysed using an Ultimate 3000 UHPLC (Thermo
157   Scientific, USA) coupled to a Q-Exactive Orbitrap MS (Thermo Fisher Scientific, USA) using data
158   dependent tandem mass spectrometry (ddMS^2) with heated electrospray ionization source (HESI).
159   The UHPLC method uses a reversed-phase 5 µm, 4.6 mm × 100 mm, polar end capped Accucore
160   column (Thermo Scientific, UK) held at 40 °C. The mobile phase consisted of water (A, optima grade)
161   and methanol (B, optima grade) both with 0.1 % (v/v) of formic acid (98 % purity, Acros Organics).
162   Gradient elution was used, starting at 90 % (A) with a 1-minute post-injection hold, decreasing to 10
163   % (A) at 26 minutes, returning to the starting mobile phase conditions at 28 minutes, followed by a
164   2-minute hold allowing the re-equilibration of the column. The flow rate was set to 0.3 mL min^{-1}. A
165   sample injection volume of 4 µL was used. The capillary and auxiliary gas heater temperatures were
166   set to 320 °C, with a sheath gas flow rate of 45 (arb.) and an auxiliary gas flow rate of 20 (arb.).
167   Spectra were acquired in the negative ionization mode with a scan range of mass-to-charge (*m/z*) 50
168   to 750. Tandem mass spectrometry was performed using higher-energy collision dissociation with a
169   stepped normalized collision energy of 10,45 and 60. The isolation window was set to *m/z* 2.0 with a
170   loop count of 10, selecting the 10 most abundant species for fragmentation in each scan.

171   A mass spectral library was built using the compound database function in Tracefinder 4.1 General
172   Quan software (Thermo Fisher Scientific, USA). To build the library, compounds from previous
173   studies (Chan et al., 2010; Nestorowicz et al., 2018; Ng et al., 2008; Riva et al., 2016b; Schindelka et

Atmospheric
Chemistry
and Physics
Discussions

174   al., 2013; Surratt et al., 2008a) were searched for in an afternoon and a night-time filter sample
175   extract analysis using the Xcalibur software. Further details can be found in Bryant et al., 2021 and
176   the SI. Isoprene and monoterpene markers were quantified using the method in Bryant et al., 2021.
177   Overall uncertainties associated with calibrations, proxy standards and matrix effects were
178   estimated. The uncertainties associated with 2-MG-OS and 2-methyl tetrol OS (2-MT-OS) were
179   calculated to be 58.9 % and 37.6 % respectively, mainly due to the large uncertainties in the matrix
180   correction factors. Isoprene SOA markers quantified by the average of 2-MT-OS and 2-MG-OS
181   calibrations have an associated uncertainty of 69.9 %. For monoterpene SOA species which were
182   quantified by camphorsulfonic acid, the associated uncertainty is estimated to be 24.8 %.

183

2.4 Supplementary measurements

185   A suite of complementary measurements were made alongside the filter collection including
186   VOCs(Stewart et al., 2021c), oxygenated-VOCs, NO_x, CO, O_3, SO_2, HONO, photolysis rates and
187   measurements of PM_1 non-refractory aerosol chemical components with a high resolution Aerosol
188   Mass Spectrometer (HR-AMS). Detailed instrument descriptions can be found in Nelson et al.,
189   (2021). Briefly, VOCs and oxygenated-VOCs were measured via two gas-chromatography (GC)
190   instruments (DC-GS-FID and GC-GC-FID). NO_x was measured via a dual channel chemiluminescence
191   analyser with fitted with a blue light converter for NO_2 (Air Quality Designs Inc., Colorado) alongside
192   CO which was measured with a resonance fluorescent instrument (Model Al5002, Aerolaser GmbH,
193   Germany). O_3 was measured as outlined by Squires et al., (2020) using an ozone analyser (49i,
194   Thermo Scientific). SO_2 was measured using a 43i SO_2 analyser (Thermo scientific). High-resolution
195   aerosol mass spectrometry measurements were conducted as outlined in Cash et al., (2021). Ion
196   chromatography measurements were undertaken by the experimental approach outlined by Xu et
197   al., (2020) as part of an intercomparison study. Briefly, filter cuttings were taken from the filter and
198   extracted ultrasonically for 30 mins in 10 mL of ultrapure water and then filtered before analysis (Xu
199   et al., 2020).

200   Meteorology data was downloaded from the NOAA Integrated Surface Database via the Worldmet R
201   package for the Indira Gandhi International Airport (code: 421810-99999) (Carslaw, D ., accessed:
202   2021). The planetary boundary layer height (PBLH) was obtained from the ERA5 (ECMWF ReAnalysis
203   5) data product at 0.25° resolution in 1-hour time steps at the position Lat 28.625˚, Lon. 77.25˚. The
204   data for both campaigns was then selected between the start time of the first filter of that
205   campaign, and the end time of the last filter of the same campaign.

3. Results

3.1 Meteorology

208   The time series for temperature, RH, planetary boundary layer height (PBLH) and ventilation
209   coefficient (VC) across the pre- and post-monsoon campaigns are shown in Figure S1. For the pre-
210   monsoon campaign, the average air temperature was (35.8 ± 4.5) °C compared to (24.7 ± 4.6) °C in
211   the post-monsoon campaign (Table S2). The pre-monsoon campaign also showed higher average
212   wind speeds, with an average of (3.8 ± 1.4) ms^{-1}, compared to (1.7 ± 1.3) ms^{-1} in the post-monsoon
213   campaign. The average RH of the pre- and post-monsoon were (39.4 ± 13.6) % and (57.3 ± 16.6) %
214   respectively, both showing similar diurnals with a minimum around mid-morning and nocturnal
215   maximum (Figure S2). The PBLH shows a similar diurnal between the two campaigns, with the
216   nocturnal boundary layer breaking down around 06:00-07:00 with a midday peak, before re-
217   establishing the nocturnal boundary layer around 19:00. The pre-monsoon PBLH has an average

218   maximum of ~2400 m compared to post-monsoon ~1700 m and a minimum of 270 m compared to
219   52 m (Figure S2). The ventilation coefficient (VC = wind speed x PBLH) has been used previously to
220   identify periods of adverse meteorological conditions and gives an idea of how stagnant atmospheric
221   conditions are and the general role of the atmosphere in the dilution of species. (Gani et al., 2019)
222   As shown in Figure S1, the conditions during the post-monsoon campaign were much more stagnant
223   than the pre-monsoon campaign. The VC was on average 4.5 times higher during the pre-monsoon
224   campaign compared to the post-monsoon campaign (Table S2) in line with previous studies (Gani et
225   al., 2019; Saha et al., 2019). The more stagnant conditions during the post-monsoon campaign likely
226   traps nocturnal emissions and their reaction products close to the surface, allowing for a significant
227   build-up of concentrations.

228   **3.2 Gas phase observations**

229   Time series of the observed mixing ratios (ppbv) of NO, NO_2 and O_3 are shown in Figure 1, for the
230   pre- and post-monsoon campaigns. The campaign averaged diurnal profiles are shown in Figure S3
231   and the mean, median and maximum mixing ratios are given in Table S2. It should be noted that only
232   one week of data was available for the pre-monsoon period. During the post-monsoon campaign,
233   extremely high mixing ratios of NO were observed with a campaign maximum mixing ratio of ~870
234   ppbv during the early morning of the 1st of November. During the early part of the pre-monsoon
235   campaign, a large enhancement in NO was observed with mixing ratios around 400 ppbv (Figure S4),
236   followed by significantly lower concentrations throughout the rest of the campaign. The campaign-
237   average NO diurnal profile shows very high NO mixing ratios at night (pre-: ~ 50 ppbv, post-: ~300
238   ppbv), with low afternoon mixing ratios < 2 ppbv due to ozone titration. These high NO
239   concentrations at night likely reduce any night-time chemistry through reactions with NO_3 radicals
240   and ozone. NO_2 during the pre-monsoon was observed to increase as the boundary layer reduced in
241   the late afternoon, with a mid-afternoon minimum. During the post-monsoon, a double peak in
242   concentrations was observed, in line with increasing ozone in the morning, and increasing NO in the
243   afternoon. Ozone showed a strong diurnal variation across both campaigns, with average afternoon
244   mixing ratios ~ 75 ppbv with pre- and post-monsoon maximums of 182 ppbv and 134 ppbv
245   respectively. Night-time O_3 concentrations were significantly higher during the pre-monsoon
246   campaign, likely due to the significantly lower NO concentrations.

247   **3.3 Particle phase observations**

248   The sampling site was heavily polluted in terms of particulate matter. The mean ± σ $PM_{2.5}$
249   concentration (Table S2) during the pre-monsoon campaign was (141 ± 31) µg m^{-3} with a spike in
250   concentrations of 672 µg m^{-3} on the 01/6/2018 at 21:00 (Figure 1). The diurnal (Figure S5) shows
251   concentrations generally flat throughout the day. During the post-monsoon campaign, the average
252    $PM_{2.5}$ concentration was higher at (182 ± 94) µg m^{-3}, with a spike in concentrations of 695 µg m^{-3} at
253   the end of the campaign (Figure 1). The diurnal shows a mid-afternoon minimum with high morning
254   and night concentrations. HR-AMS was used to measure the PM_1 sulfate and total organics.
255   Campaign averaged total organics concentrations were approximately double in the post-monsoon
256   (48.7 ± 35.4) µg m^{-3} compared to the pre-monsoon (19.8 ± 13.7) µg m^{-3}. During the pre-monsoon
257   campaign, concentrations are generally flat throughout the day, with an increase in the late
258   afternoon, likely as the boundary layer decreases (Figure S5). During the post-monsoon, a much
259   more prominent diurnal is observed, with a mid-day minimum and high night-time concentrations.
260   This diurnal is likely driven by boundary layer conditions. Sulfate averaged (7.5 ± 1.8) µg m^{-3} during
261   the pre-monsoon campaign, with slightly lower average concentrations observed in the post-
262   monsoon: (5.6 ± 2.7) µg m^{-3} as shown in Figure S5. The sulfate diurnal variations are similar to those
263   of the organic aerosol.

264

265

266

267

268

269

270

271

272

273

274

275

276

277

278

279

280

281

283

284

285

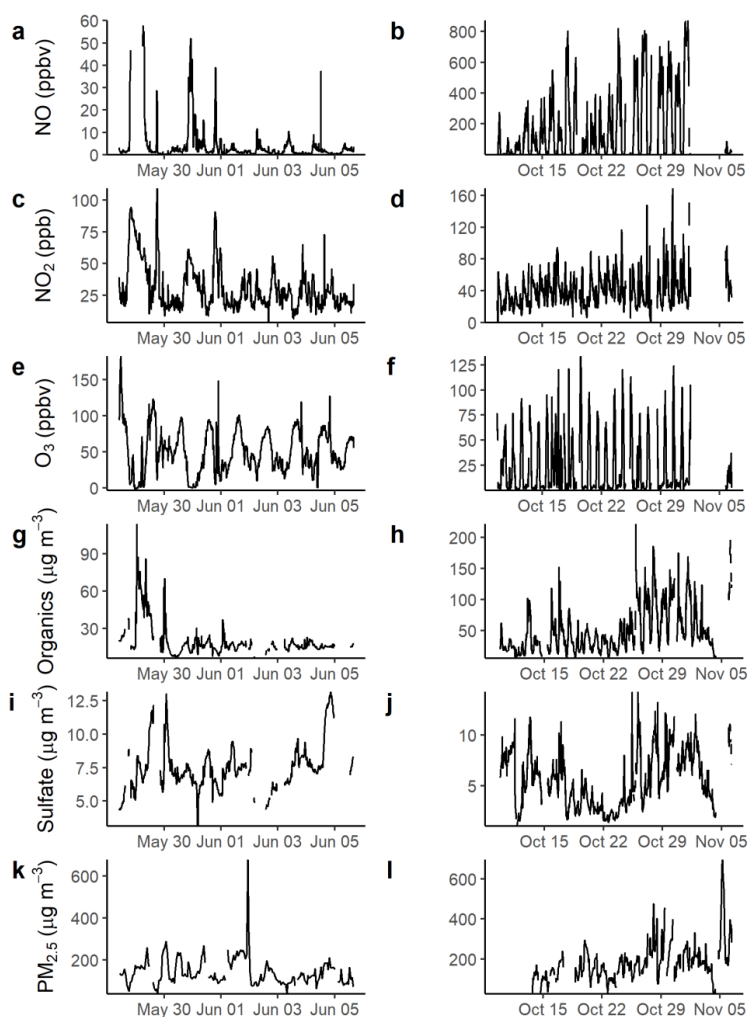286

287

288

289

290

291

Figure 1. Time series of pollutants across the pre- (a,c,e,g,i) and post-monsoon (b,d,f,h,j) campaigns. During the pre-monsoon, NO concentrations were filters to below 60 ppbv, due to a large enhancement in concentrations at the start of the campaign, the full time series is shown in Figure S4. NO, NO₂, O₃ and HR-AMS – SO₄²⁻ were averaged to 15 minutes. PM₂.₅ was measured hourly.

294

295

296

297

298   **3.4 Isoprene and monoterpene measurements**

299   Isoprene was measured hourly using gas-chromatography with flame-ionisation-detection (GC-FID)
300   across the two campaigns (Nelson et al., 2021), with the time series shown in Figure 2. The time
301   series highlights similar diurnal variability each day, driven by biogenic emissions. Figure 3 shows the
302   average diurnal profiles of isoprene during pre-monsoon (a) and post-monsoon (b). The mean
303   isoprene mixing ratios were (1.22 ± 1.28) ppbv and (0.93 ± 0.65) ppbv, with maximum isoprene
304   mixing ratios of 4.6 ppbv and 6.6 ppbv across the pre- and post-monsoon, respectively. This is in the
305   same range as measured in Beijing (winter mean: (1.21 ± 1.03) ppbv, summer mean: (0.56 ± 0.55)
306   ppbv, Acton et al., (2020)), Guangzhou (year round (1.14) ppbv) (Zou et al., 2019) and Taipei
307   (summer daytime: (1.26) ppbv, autumn daytime: (0.38) ppbv) (Wang et al., 2013). The diurnal
308   variability observed in the pre-monsoon period corresponds to a typical biogenic emission driven
309   profile, with a rapid increase of isoprene around 05:00, reaching a peak around or after midday,
310   before a nocturnal minimum. Figure 3 indicates that average daytime peak isoprene mixing ratios
311   during the pre-monsoon campaign were roughly double that of the post-monsoon campaign. In
312   contrast, average nocturnal mixing ratios of isoprene were 5 times higher in the post-monsoon
313   compared to the pre-monsoon ((0.65 ± 0.43) ppbv versus (0.13 ± 0.18) ppbv). In the post-monsoon
314   campaign, isoprene mixing ratios show a strong biogenic emission driven diurnal profile at the start
315   of the campaign. However, towards the end of the post monsoon measurement period, the isoprene
316   mixing ratios become less variable with a high mixing ratio maintained overnight (Figure 2). This is
317   potentially due to more stagnant conditions as observed by the VC in Figure S1.

318

319

320

321
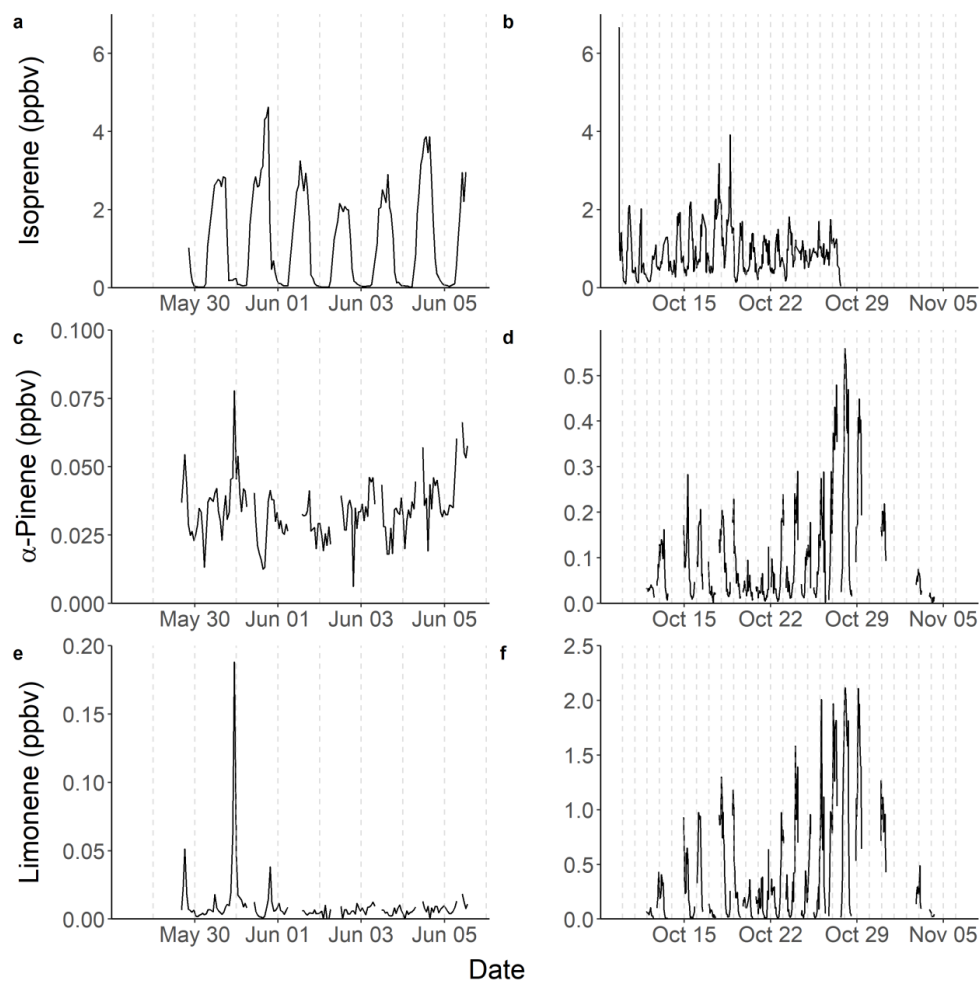
322

323

324

325

326

327

328

329

330

331

332

Figure 2. Time series across the pre- (left) and post-monsoon (right) campaigns of Isoprene (a,b), α-pinene (c,d), limonene (d,e). The vertical dotted lines represent midnight for each day.

A recent study in Delhi averaged across post-monsoon, summer and winter campaigns found that at vegetative sites biogenic isoprene contributed on average 92 - 96 % to the total isoprene, while at traffic dominated sites only 30 − 39 % of isoprene was from biogenic sources (Kashyap et al., 2019). This is similar to the contributions of biogenic isoprene (40 %) to total isoprene mixing ratios at the traffic dominated Marylebone Road London site.(Khan et al., 2018a) To gain some understanding of the sources of isoprene at our site in Delhi, the observed concentrations of isoprene were correlated to CO, which is an anthropogenic combustion tracer (Figure 4) similar to previous studies.(Khan et

344 al., 2018a; Wagner and Kuttler, 2014) The isoprene concentrations were split between night and day
345 (pre-monsoon; night: 19:00 – 05:00 h, day 05:00 – 19:00 h, post-monsoon; night: 17:00-06:00 h, day:
346 06:00-17:00 h), based on the observed isoprene diurnals as shown in Figure 3. Isoprene correlated
347 strongly with CO during the night across both campaigns (pre-monsoon: R^2= 0.69, post-monsoon:
348 R^2= 0.81), but no correlation was observed during the day ($R^2 < 0.1$). This suggests that daytime
349 isoprene is predominantly from biogenic sources, although a small amount will be from
350 anthropogenic sources, and that nocturnal isoprene is emitted from anthropogenic sources, as seen
351 in other locations. (Khan et al., 2018b; Panopoulou et al., 2020; Wang et al., 2013) The night-time
352 isoprene mixing ratios (pre-monsoon: (0.13 ± 0.18) ppbv, post-monsoon: (0.65 ± 0.43) ppbv) were
353 substantially higher than measured previously in Beijing and London (<50pptv, (Bryant et al., 2020;
354 Khan et al., 2018b)), but pre-monsoon concentrations were similar to those observed at night in
355 Taipei (0.19 ppbv)(Wang et al., 2013). The high night-time concentrations during the post-monsoon
356 period, towards the end of October are also likely influenced by the formation of a very low
357 boundary layer, trapping pollutants near the surface, affecting all species similarly. An increase in
358 biomass burning may also be a factor. Therefore, during the post-monsoon campaign a significant
359 amount of isoprene oxidation products will be of anthropogenic origin.
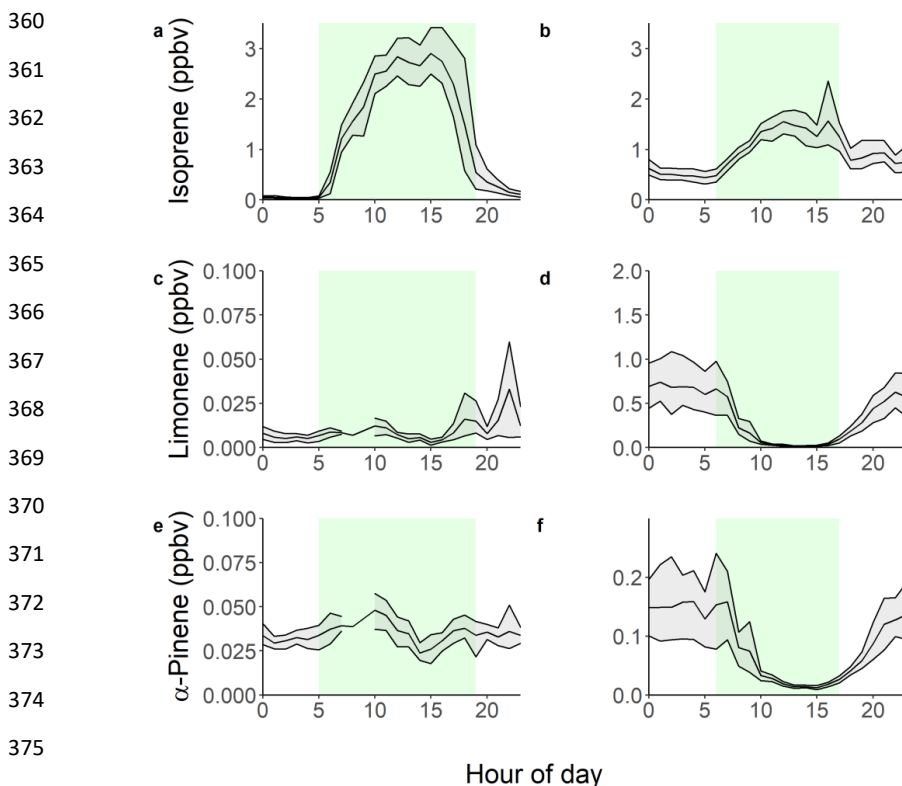
Figure 3. Diurnal variations across the pre (left) and post-monsoon (right) campaigns of Isoprene (a,b), limonene (c,d) and α-pinene (e,f). The grey shaded area represents the 95 % confidence interval. The green shaded area represents the times driven by biogenic emissions, as defined by the isoprene diurnals.

380

381

382 Several monoterpenes were measured using GCxGC-MS. The time series of two monoterpenes,
383 limonene and α-pinene, are shown in Figure 2. The α-pinene mixing ratio averaged (0.034 ± 0.011)
384 ppbv during the pre-monsoon and (0.10 ± 0.11) ppbv during the post monsoon periods. This is in
385 comparison to limonene, which averaged (0.01 ± 0.02) ppbv and (0.42 ± 0.51) ppbv across the pre-
386 and post-monsoon campaigns, respectively. A strong diurnal variation was observed for both
387 monoterpenes during the post-monsoon, peaking during the night (Figure 3), with a midday
388 minimum. Nocturnal mixing ratios of the two monoterpenes were substantially higher during the
389 post-monsoon (Limonene: (0.59 ± 0.11) ppbv, α-pinene: (0.13 ± 0.12) ppbv) than the pre-monsoon
390 (Limonene: (0.011 ± 0.025) ppbv, α-pinene: (0.033 ± 0.009) ppbv) period. This diurnal again is likely
391 driven by boundary layer dynamics. During the pre-monsoon, limited diurnal variability was
392 observed compared to the post-monsoon. Limonene was dominated by 3 short lived spikes in
393 concentrations towards the start of the campaign (Figure 2). α-pinene concentrations generally
394 increased during the morning, before decreasing during the afternoon. A further 10 monoterpenes
395 were measured concurrently using GCxGC-MS (Nelson et al., 2021; Stewart et al., 2021c). For all MT
396 species, the post monsoon period had higher mean mixing ratios, with large nocturnal
397 enhancements in mixing ratios.

398 During the post-monsoon, α-pinene and limonene correlated strongly with CO during the day (α-
399 pinene; R^2 = 0.82, limonene; R^2 = 0.90) and moderately at night (α-pinene; R^2 = 0.49, limonene; R^2 =
400 0.56) as shown in Figure 4, suggesting anthropogenic sources. Other potentially important
401 anthropogenic monoterpene sources include biomass burning, cooking and the use of personal
402 care/volatile chemical products (Coggon et al., 2018; Gkatzelis et al., 2021; Hatch et al., 2019; Klein
403 et al., 2016). The shallow nocturnal boundary layers across both campaigns leads to relatively high
404 concentrations of total monoterpenes, with a maximum mixing ratio of 6 ppbv observed during the
405 post-monsoon (Stewart et al., 2021c). After sunrise, the expanding boundary layer dilutes the high
406 concentrations alongside increasing OH concentrations from photolytic sources such as the
407 photolysis of HONO and carbonyls which likely causes a rapid decrease in the monoterpene mixing
408 ratios.

409

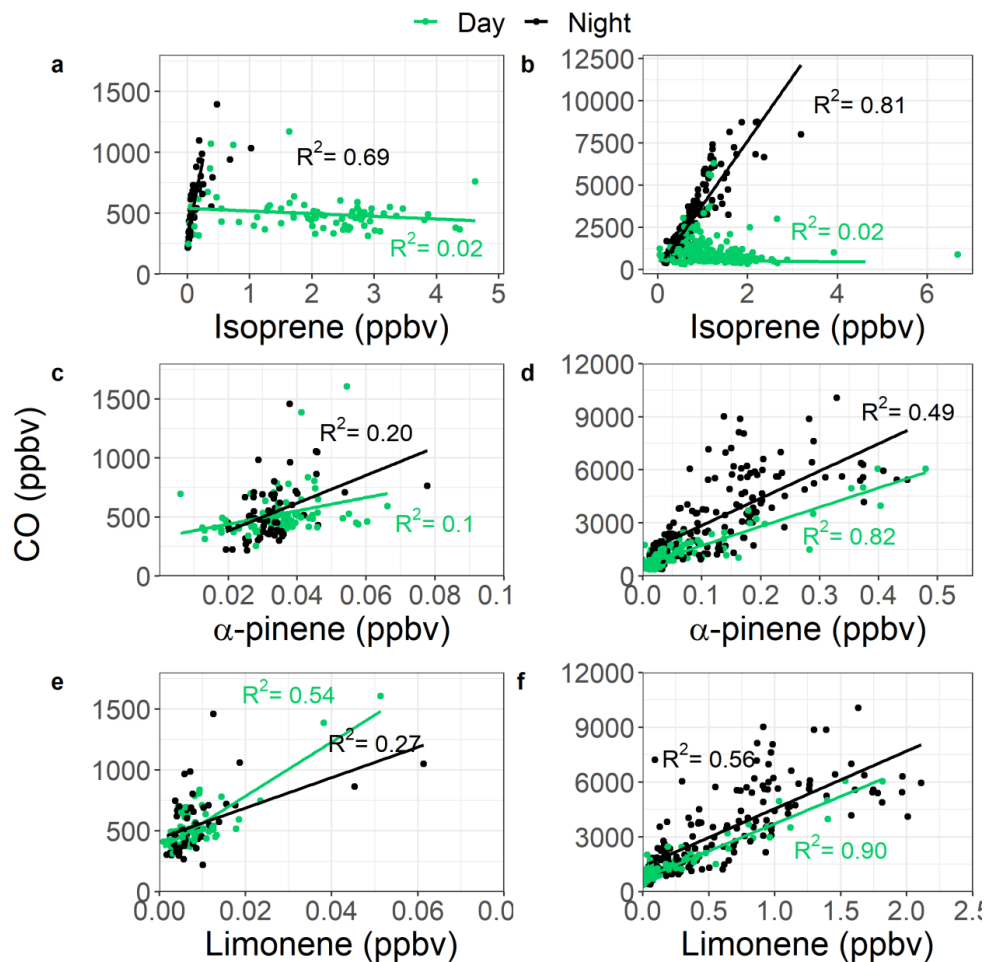410

411

412

413

414

415

416

417

418

419

420

421

Figure 4. Correlations between Isoprene, limonene and α-pinene with CO across the pre (left) and post-monsoon (right) campaigns. The samples are split between daytime (green) and night-time (black) as defined by the Isoprene diurnals in Figure 3.
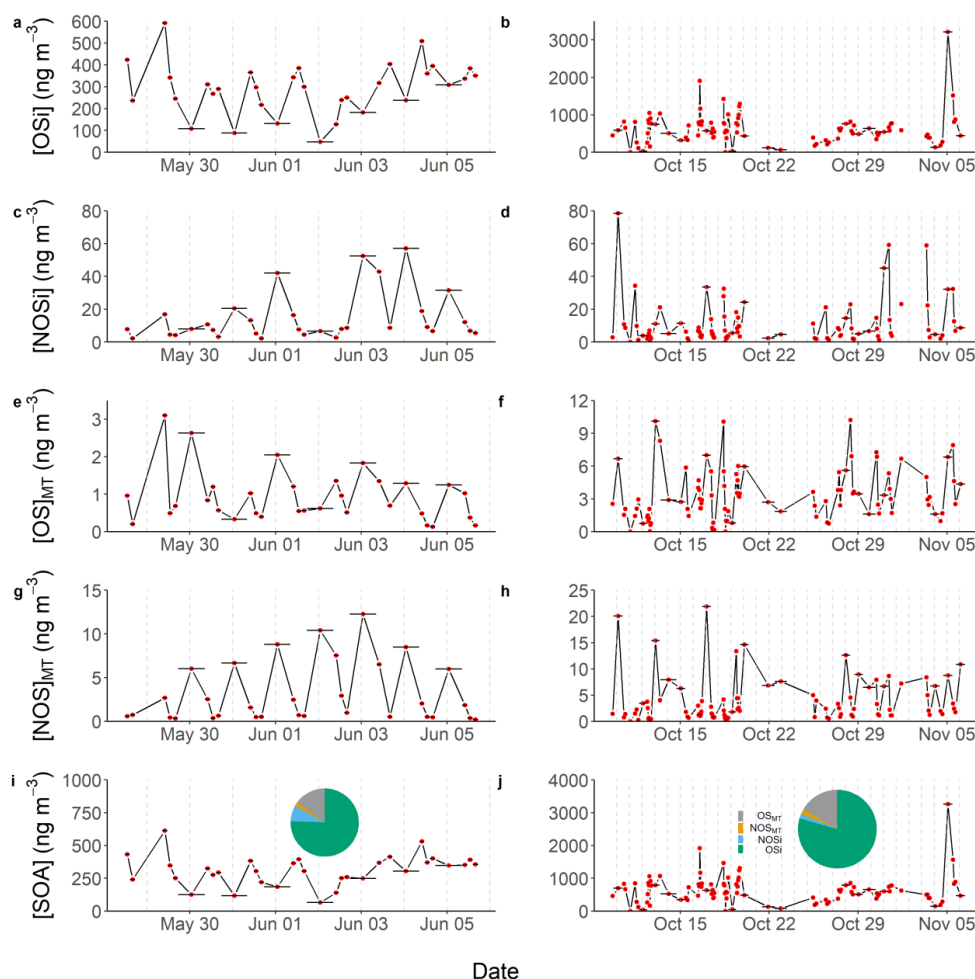
422

423

424

425

426

427

428

429

430

431

432

Figure 5. Time series across the pre- (left) and post-monsoon (right) campaigns of the quantified SOA tracers: OSi (a,b), NOSi (c,d), OS_{MT} (e,f), NOS_{MT} (g,h) and the sum of all SOA tarcers (i,j) with the average campaign contributions. The vertical dotted lines represent midnight for each day. Only species identified in more than 40 % of the samples for each campaign were included.

436

437

438

439

440 **3.5 Secondary organic aerosol formation**

Atmospheric
Chemistry
and Physics
Discussions

Open Access

EGU

441 At the measured concentrations, monoterpenes and isoprene are an important source of ozone and
442 OH reactivity at this site (Nelson et al., 2021). The resultant oxidised products will also be a key
443 source of SOA production. The UHPLC-MS^2 analysis identified and quantified 75 potential markers
444 across four classes of SOA, isoprene OS (OSi) and NOS (NOSi) derived species and monoterpene OS
445 (OS$_{MT}$) and NOS (NOS$_{MT}$) species. Figure 5 shows the contribution to the total quantified SOA (qSOA),
446 which consists of the time averaged sum of the four SOA classes (OSi, NOSi, OS$_{MT}$, NOS$_{MT}$), across the
447 pre- and post-monsoon campaigns. OSi species were the dominant SOA class quantified in this
448 study, contributing 75.6 % and 79.4 % of the qSOA across the pre- and post-monsoon campaigns
449 respectively. NOSi species contributed significantly more to the qSOA during the pre-monsoon (7.6
450 %) compared to the post-monsoon (2.1 %) period. Similar contributions from the monoterpene
451 derived SOA species were observed across both campaigns.

452 **3.5.1 Isoprene SOA**

453 OSi species are predominantly formed by photo-oxidation of isoprene by OH radicals with the
454 subsequent products formed dependent on ambient NO concentrations (Wennberg et al., 2018).
455 The pathways are split into high-NO and low-NO, although the NO concentrations that constitute
456 high and low are a sliding scale depending on the amount of reactivity (defined as ([OH] x k_{OH})
457 (Newland et al., 2021). Under low-NO conditions, isoprene epoxydiol isomers (IEPOX) (Paulot et al.,
458 2009) are formed which can then undergo reactive uptake to the particle phase by acid-catalysed
459 multiphase chemistry involving inorganic sulfate, to form 2-MT-OS (Lin et al., 2012; Riva et al., 2019;
460 Surratt et al., 2010). Under high-NO conditions, 2-methyl glyceric acid is the dominant gas-phase
461 marker produced, which can undergo reactive uptake to the particle phase to form 2-MG-OS (Lin et
462 al., 2013a; Nguyen et al., 2015; Surratt et al., 2006, 2010).

463 A total of 21 potential OSi C$_{2-5}$ markers previously identified in chamber studies (Nguyen et al., 2010;
464 Riva et al., 2016a; Surratt et al., 2007, 2008b) and other ambient studies (Bryant et al., 2020;
465 Budisulistiorini et al., 2015; Hettiyadura et al., 2019; Kourtchev et al., 2016; Rattanavaraha et al.,
466 2016a; Wang et al., 2018b, 2021b) were quantified in the collected ambient samples. It should be
467 noted that several of the smaller (C$_{2-3}$) OSi tracers likely form from glyoxal, methylglyoxal and
468 hydroxyacetone as well as isoprene, and as such present a potential non-isoprene source of OSi
469 (Galloway et al., 2009; Liao et al., 2015).

470 Figure 5 shows the time series of total OSi concentrations observed across pre- (left, 5a) and post-
471 (right, 5b) monsoon campaigns. Total OSi time averaged concentrations (Table 1) were c.a. 2.3 times
472 higher during the post-monsoon (~556.6 ± 422.5 ng m^{-3}) campaign than the pre-monsoon campaign
473 (~237.8 ± 118.4 ng m^{-3}). These concentrations are similar to those observed in Beijing during summer
474 2017 (237.1 ng m^{-3}, (Bryant et al., 2020)), but higher than those observed in Shanghai in 2018 (40.4
475 ng m^{-3}) and 2019 (34.3 ng m^{-3}) (Wang et al., 2021b). As previously discussed, OSi species have been
476 shown to form via the gas-phase photo-oxidation of isoprene, with the reactive update of the
477 oxidised species into to particulate phase via sulfate (Lin et al., 2013a; Surratt et al., 2010). Recently,
478 a heterogeneous photo-oxidation pathway from 2-MT-OS (C$_5$H$_{12}$O$_7$S) to several OSi species was
479 proposed, including C$_5$H$_{10}$O$_7$S, C$_5$H$_8$O$_7$S, C$_5$H$_{12}$O$_8$S, C$_5$H$_{10}$O$_8$S and C$_4$H$_8$O$_7$S (Chen et al., 2020). 2-MT-OS
480 showed moderate correlations (pre-monsoon : R^2 = 0.52-0.72, post-monsoon: R^2 = 0.14-0.35) with
481 these OSi tracers that were lower than observed in Beijing summer (R^2 = 0.83-0.92) (Bryant et al.,
482 2020). These correlations could suggest that this is a more common formation route in pre-monsoon
483 Delhi, than in post-monsoon. However, the correlations could also be driven by the common
484 pathways between the OSi species, with the reactive uptake of gas phase intermediates via sulfate
485 reactions. The lower correlations during the post-monsoon could be due to increased influences of
486 anthropogenic sources coupled to the stagnant conditions.

487 Figure 6 shows the binned OSi concentrations for each filter collection time across the pre- and post-
488 monsoon campaigns to create a partial diurnal profile. During the pre-monsoon, the daily variation
489 in OSi concentrations was much clearer, with day-time maxima and nocturnal minima, which are in
490 line with daily peak isoprene (Figure 3) and OH radical concentrations. The highest observed OSi
491 concentrations during the pre-monsoon were ~ 600 ng m^{-3}, which occurred at the start of the
492 campaign. High isoprene concentrations may have been the cause, but unfortunately isoprene
493 measurements were not available during this period to confirm. However, high OSi concentrations
494 also occurred when particulate inorganic sulfate concentrations were at their highest (Figure S6),
495 while sulfate measured via the HR-AMS was also high during this period (Figure 1). During the post-
496 monsoon, although a similar diurnal pattern was observed, the variation was less pronounced, with
497 higher OSi concentrations observed at the start and end of the campaign (Figure 5). The low OSi
498 concentrations during the middle of the campaign, coincide with lower isoprene and inorganic
499 sulfate concentrations, but also low VC values, suggesting more stagnant conditions.

500 The sum of OSi species across all filters sampled showed a variable correlation with particulate
501 sulfate across both campaigns. The pre-monsoon correlation was similar to those observed in
502 Beijing, Guangzhou and the SE-US (R^2: 0.55)(Bryant et al., 2020, 2021; Budisulistiorini et al., 2015;
503 Rattanavaraha et al., 2016a) while the post-monsoon was significantly weaker (R^2: 0.28). However, a
504 clear relationship between OSi tracers and inorganic sulfate can be seen in Figure 7 across both
505 campaigns, where the highest OSi concentrations occurred under the highest SO$_4^{2-}$ concentrations.
506 During the post-monsoon campaign, OSi concentrations levelled off at high sulfate concentrations.
507 In the pre-monsoon this levelling off is not observed, potentially due to the lower number of
508 samples. The high concentrations of organics measured by the HR-AMS (Table S2) during the post-
509 monsoon (48.7 ± 35.4) µg m^{-3} compared to the pre-monsoon (19.8 ± 13.7) µg m^{-3}, suggests the
510 reactive uptake of the gaseous OSi intermediates to the aerosol phase may be limited due to
511 extensive organic coatings on the sulfate aerosol. Multiple studies have now shown that organic
512 coatings on sulfate aerosol can limit the reactive uptake of IEPOX, suggesting the pre-monsoon is
513 volume limited but the post-monsoon is diffusion limited. (Gaston et al., 2014; Lin et al., 2014; Riva
514 et al., 2016c)

515 Isoprene NOS (NOSi) have been shown to be produced by photo-oxidation in the presence of NO
516 and from NO$_3$ oxidation chemistry (Hamilton et al., 2021; Ng et al., 2017; Surratt et al., 2008b). Ten
517 different NOSi tracers were screened for across the two campaigns, with eight identified in the pre-
518 monsoon and ten in the post-monsoon. These tracers included: mono-nitrated (C$_5$H$_9$O$_{10}$NS,
519 C$_5$H$_{11}$O$_9$NS, C$_5$H$_{11}$O$_8$NS), di-nitrated (C$_5$H$_{10}$O$_{11}$N$_2$S), and tri-nitrated (C$_5$H$_9$O$_{13}$N$_3$S) species. These tracers
520 have been identified previously in China (Bryant et al., 2020, 2021; Hamilton et al., 2021; Wang et
521 al., 2018b, 2021b). Unlike the OSi tracers, total NOSi concentrations were on average higher during
522 the pre-monsoon (32.6 ± 19.9) ng m^{-3} compared to the post-monsoon (20.2 ± 13.3) ng m^{-3}. This is
523 likely due to extremely high night-time NO concentrations during the post-monsoon quenching NO$_3$
524 radicals, limiting the isoprene + NO$_3$ pathway. The NOSi time series and diurnal shown in Figures 5
525 and 6 respectively highlight the strong nocturnal enhancements in concentrations during the pre-
526 monsoon, suggesting isoprene + NO$_3$ formation pathway is dominant. Due to the long sampling time,
527 it is likely that these species are forming in the early evening as NO$_3$ oxidation becomes more
528 competitive with OH, while isoprene concentrations are still relatively high. During the post-
529 monsoon, NOSi concentrations were highest at night and the early morning. The high morning
530 concentrations could be due to non-local sources mixing down as the shallow night-time boundary
531 layer breaks down. Ideally, future work in Delhi or India should focus on the measurements of
532 radicals and OH reactivity (k_{OH}), in order to improve our understanding of the chemistry occurring in
533 extremely polluted environments. A large spike in NOS$_i$ concentrations is observed at the start of the

534   post-monsoon campaign, which was not observed for the OS_i tracers, this coincides with lower NO
535   concentrations than the rest of the post-monsoon campaign, reducing the NO_3 quenching by NO,
536   allowing for more isoprene + NO_3 oxidation. The NOSi species did not correlate towards particulate
537   sulfate ($R^2 < 0.2$) across either campaign, suggesting that uptake onto sulfate is not the limiting step
538   in NOSi formation (unlike for the OSi species).

539

540

541

542
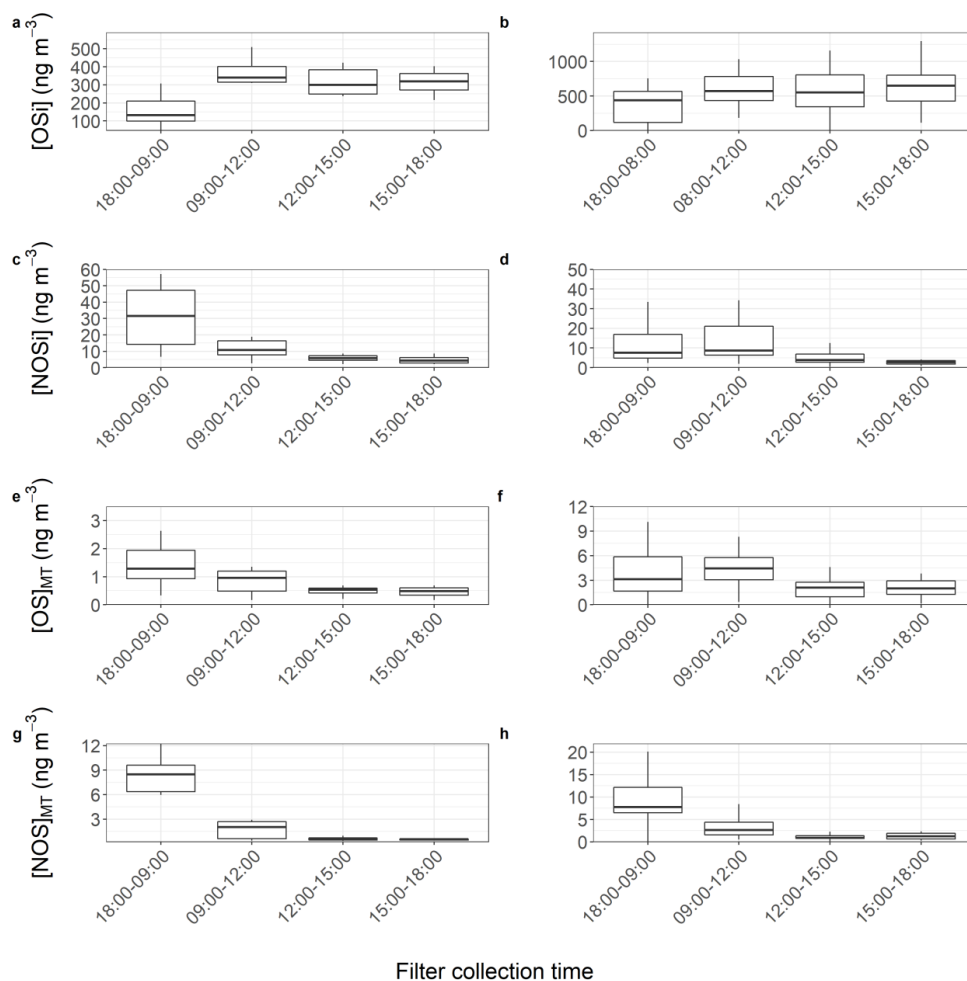
Filter collection time

Figure 6. Partial diurnal variations from the binned concentrations of OSi, NOSi, OS_{MT} and
NOS_{MT} concentrations at each filter collection time across the pre (left) and post-monsoon
(right) campaigns. The lower and upper part of the box representing the 25th and 75th
percentiles, with the upper and lower lines extending no further than 1.5 times the
interquartile range of the highest and lowest values within the hinge respectively. Only
species identified in more than 40 % of the samples for each campaign were included.

16
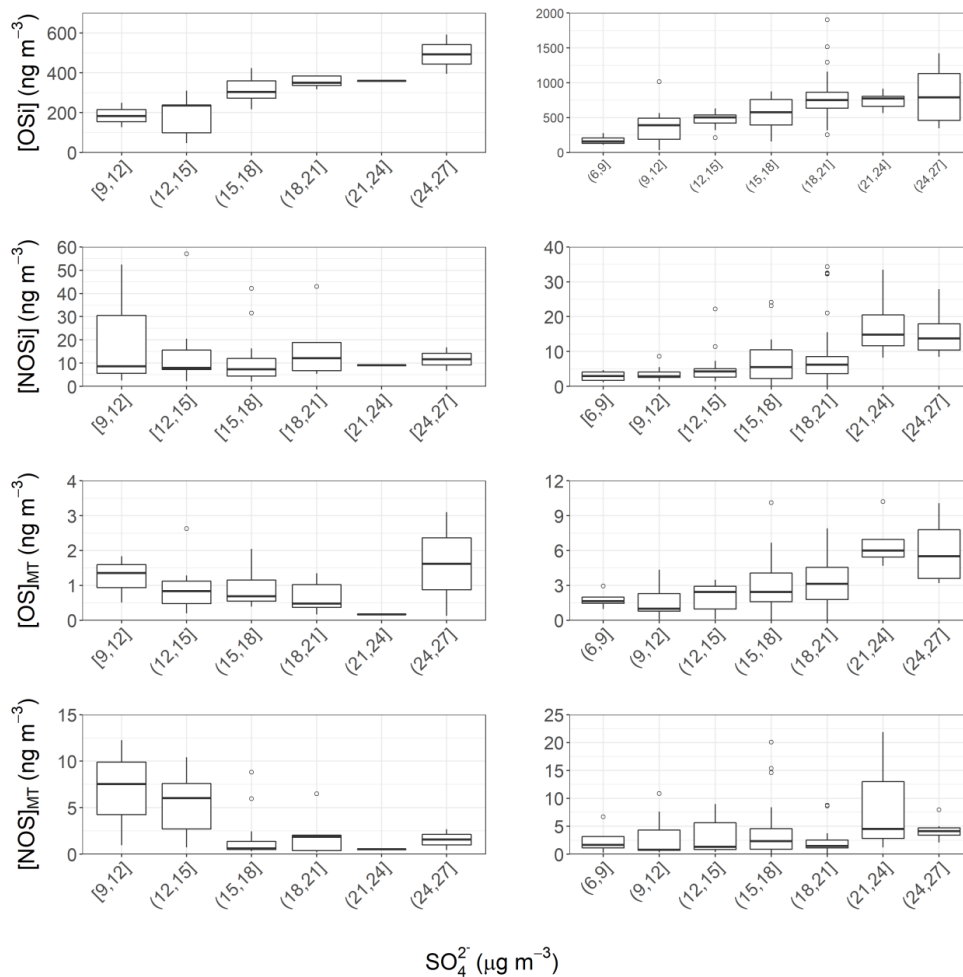
Figure 7. Quantified SOA (OS$_i$, NOS$_i$, OS$_{MT}$, NOS$_{MT}$) vs inorganic sulfate concentrations across the pre- (left) and post-monsoon (right) campaigns. The lower and upper part of the box representing the 25th and 75th percentiles, with the upper and lower lines extending no further than 1.5 times the interquartile range of the highest and lowest values within the hinge respectively. Only species identified in more than 40 % of the samples for each campaign were included.

556

3.8 Monoterpene secondary organic aerosol

Monoterpene derived OS (OS_{MT}) and NOS (NOS_{MT}) markers have also been identified from the oxidation by OH, NO_3 and O_3 in the presence of SO_2 or sulfate seed in simulation studies (Brüggemann et al., 2020b; Iinuma et al., 2007; Kleindienst et al., 2006; Surratt et al., 2008a; Zhao et al., 2018). Compared to isoprene, the ozonolysis of monoterpenes is a key degradation pathway, with higher SOA yields from ozonolysis observed when compared to isoprene (Åsa M. Jonsson et al., 2005; Atkinson and Arey, 2003; Eddingsaas et al., 2012a, 2012b; Kristensen et al., 2013; Mutzel et al., 2016; Simon et al., 2020; Zhao et al., 2015). A recent study in the SE-US suggests that the degradation of 80 % of monoterpenes at night is due to ozonolysis at that location (Zhang et al., 2018). Monoterpene derived OS and NOS species have been extensively observed, with ON contributing considerably to OA (Lee et al., 2016; Xu et al., 2015; Zhang et al., 2018). Recently NOS hydrolysis has also been shown to be a potential formation route of OS particle phase species (Darer et al., 2011; Passananti et al., 2016).

Twenty-three monoterpene-derived organosulfate (OS_{MT}) species, which have been seen previously in chamber (Surratt et al., 2008b) and ambient studies (Brüggemann et al., 2019; Wang et al., 2018b, 2021b), were identified across the pre- and post-monsoon campaigns. It should be noted that recently OS_{MT} artefacts has been shown to form when filters have been sampled without a denuder. (Brüggemann et al., 2020b). However, the strong diurnal variations of the OS_{MT} species, and lack of correlation with SO_2 suggest this process is unlikely to have contributed significantly to the OS_{MT} measured in this study. Post-monsoon concentrations were similar (3.96 ± 1.6) ng m^{-3} to the pre-monsoon (3.05 ± 1.3) ng m^{-3}, with $C_9H_{16}O_6S$ the dominant species across both campaigns, contributing on average ~ 29 % of the OS_{MT} mass. It should be noted that the majority of the OS_{MT} were not identified in every sample, and as such only tracers which were identified in at least 40 % of the samples were examined further.

Total OS_{MT} showed a strong diurnal profile across both campaigns, peaking at night, with an afternoon minimum (Figures 5 & 6). During the pre-monsoon campaign, the highest OS_{MT} concentrations were observed during a day-time sample, coinciding with peak sulfate and NO concentrations. Both limonene and α-pinene also show peaks during this filter sampling period of ~ 0.05 ppbv. Spikes in limonene and α-pinene concentrations were also observed on the 31st of May, but OS_{MT} concentrations were much lower, likely due to the lower sulfate concentrations. During the post-monsoon campaign, nocturnal enhancements are observed (Figure 6), suggesting MT + NO_3 chemistry is important. Like the NOSi markers, higher OS_{MT} concentrations were observed during the early morning sample, likely due to a lower PBLH concentrating the markers coupled to MT+OH/O_3 occurring after sunrise in the post-monsoon. The night-time formation of the OS_{MT} species is in line with previous studies (Bryant et al., 2021), and with the diurnal variations of α-pinene and limonene, which peak at night. Previous chamber studies investigating reactions of monoterpenes with NO_3 radicals have also shown formation of OS_{MT} with the same molecular formulae as measured here (Surratt et al., 2008a).

OS_{MT} concentrations observed in Delhi are much lower than those of the OSi, similar to other studies (Hettiyadura et al., 2019; Wang et al., 2018b, 2021b). Considering the high concentrations of extremely reactive α-pinene and limonene observed during the post-monsoon period, higher OS_{MT} concentrations might be expected. One possible reason for the low OS_{MT} is the inability of OS_{MT} precursor species to undergo reactive uptake into the aerosol phase under atmospherically relevant acidic conditions, with chamber studies suggesting extremely acidic conditions are needed for

601 uptake to occur (Drozd et al., 2013). Delhi is characterised by large concentrations of free ammonia
602 and alkaline dust, and previous studies have highlighted that it has less acidic aerosol (pH 5.7 – 6.7,
603 Kumar et al., 2018) across the year than Beijing (pH 3.8 – 4.5, Ding et al., 2019) and the SE-US (pH 1.6
604 – 1.9, Rattanavaraha et al., 2016a).

605 Unlike the OS_{MT} species, the NOS_{MT} species ($C_{10}H_{17}NO_7S$, $C_9H_{15}NO_8S$, $C_{10}H_{17}NO_9S$, $C_9H_{15}NO_9S$,
606 $C_{10}H_{17}NO_8S$) showed strong seasonality, with pre- and post-monsoon concentrations of (7.6 ± 3.8) ng
607 m^{-3} and (17.6 ± 6.1) ng m^{-3} respectively. This is opposite to the quantified NOSi species, which
608 showed higher pre-monsoon concentrations. This is likely due to much higher post-monsoon
609 concentrations of monoterpenes. Of the NOS_{MT} species observed, $C_{10}H_{17}NO_7S$ was the most
610 abundant, contributing on average 79 % and 76 % of the NOS_{MT} concentrations across the pre- and
611 post-monsoon respectively. Previous studies have also highlighted $C_{10}H_{17}NO_7S$ to be the dominant
612 monoterpene derived sulfate containing tracer (Wang et al., 2018b). In the post-monsoon nine
613 $C_{10}H_{17}NO_7S$ isomers were observed, and seven in the pre-monsoon. The summed $C_{10}H_{17}NO_7S$
614 concentrations during the pre- (5.96 ± 3.33) ng m^{-3} and post-monsoon (13.36 ± 4.98) ng m^{-3}, are of a
615 similar magnitude to those observed in other locations as shown in Table 2. These concentrations
616 are also similar to those quantified by authentic standards across four Chinese megacities (Wang et
617 al., 2021a). Like the OS_{MT} species, some NOS_{MT} species were not identified in many of the filter
618 samples, and as such tracers which were observed in more than 40 % of the samples were summed
619 for further analysis. The NOS_{MT} pre-monsoon time series (Figure 5) shows a similar temporal profile
620 to the NOSi species, with lower concentrations during the enhancement in NO concentrations
621 (Figure S4) at the start of the campaign. NOS_{MT} showed strong diurnal variations across both
622 campaigns (Figure 6), peaking at night with lower concentrations during the afternoon, as seen
623 previously (Bryant et al., 2021; Wang et al., 2018b). Therefore, the formation of NOS_{MT} is likely
624 dominated by NO_3 radical chemistry. Both NOS_{MT} and OS_{MT} species showed limited correlation
625 towards SO_2 and particulate sulfate ($R^2 < 0.1$), indicating that although sulfate is essential to their
626 formation, sulfate availability does not control NOS_{MT} concentrations.

627

628 **3.10 Contributions of total quantified SOA (qSOA) to particulate mass**

629 Particulate concentrations in Delhi are among the highest across the world (WHO, 2018), with
630 concentrations over 600 μg m^{-3} being observed during this study. qSOA, defined here as the sum of
631 all OSi, NOSi, OS_{MT}, and NOS_{MT} tracers quantified (including those not identified in more than 40 % of
632 the samples), was calculated to determine the total contribution these species make to particulate
633 mass in Delhi. Total oxidised organic aerosol (OOA), a proxy for SOA in PM_1, was derived from the
634 HR-AMS measurements during the pre- and post-monsoon campaigns, with averages of (19.8 ± 13.7)
635 μg m^{-3} and (48.7 ± 35.4) μg m^{-3} respectively. qSOA contributed on average (2.0 ± 0.9) % and (1.8 ±
636 1.4) % to the total OOA. Isoprene and monoterpene derived species contributed on average 83.2 %
637 and 16.8 % of qSOA across the pre-monsoon respectively compared to 81.5 % and 18.5 % during the
638 post-monsoon respectively. During certain periods qSOA contributed a maximum of 4.2 % and 6.6 %
639 to OOA during the pre- and post-monsoon, respectively. This is under the assumption that when the
640 OS and NOS species fragment in the AMS ion source they lose their sulfate and nitrate groups. This is
641 similar to the contributions made by OSi markers in Beijing to total OOA (2.2 %) (Bryant et al., 2020).
642 Previous studies in the SE-US have reported much higher contributions of isoprene species to total
643 OA. As quantified by an aerosol chemical speciation monitor, summed iSOA tracers on average
644 accounted for 9.4 % of measured OA at Look Rock, downwind of Maryville and Knoxville, but up to a
645 maximum of 28.1 % (Budisulistiorini et al., 2015). This is lower than that measured at a rural site at

646 Yorkville, Georgia with just low-NO isoprene SOA tracers accounting for between 12-19 % of total OA
647 (Lin et al., 2013b).

648 Sulfate was also measured in the PM_1 size range by HR-AMS, with pre- and post-monsoon mean
649 concentrations of (7.5 ± 1.8) µg m^{-3} and (5.5 ± 2.7) µg m^{-3}. The sulfate containing OS and NOS species
650 quantified in this study may fragment in the AMS to produce a sulfate signal which is not related to
651 inorganic sulfate. To estimate the contribution that sulfate contained within qSOA species could
652 make to total AMS sulfate, the quantified mass of sulfate contained within each marker was
653 calculated based on the fraction of sulfate to each marker molecular mass. For example, 2-MT-OS
654 has an accurate mass of *m/z* 216.21, meaning the percentage of 2-MT-OS mass associated with
655 sulfate is ~44 %. During the pre-monsoon campaign the qSOA sulfate accounted for on average 2.2
656 % to the total PM_1 sulfate, but up to 4.8 % on certain days. qSOA contributed considerably more to
657 the sulfate in the post-monsoon campaign, with an average of (6.1 ± 4.5) % with a maximum of 18.7
658 %. This finding indicates the need to consider the sources of particulate sulfate measured by the
659 AMS when calculating aerosol pH. The sulfate contribution from the fragmentation of common small
660 OS compounds (hydroxymethylsulfonate, methylsulfonic acid) can be distinguished in the AMS using
661 the relative ratio of sulfur containing peaks.(Chen et al., 2019; Javed et al., 2021) However, more
662 work is needed to determine how larger OS and NOS fragment in the AMS such as those quantified
663 in this study. Overall, this highlights that isoprene and MT oxidation can make significant
664 contributions to organic and sulfate-containing aerosol, even in extremely polluted environments
665 such as Delhi. It should be noted that this is just a subset of potentially many more SOA from
666 isoprene and monoterpene markers and only focusses on sulfate containing species.

667

668 Conclusion

669 Isoprene- and monoterpene-derived organosulfate (OS) and nitrooxy organosulfate (NOS) species
670 were quantified during pre- and post-monsoon measurement periods in the Indian megacity of
671 Delhi. An extensive dataset of supplementary measurements was obtained alongside filter samples,
672 including isoprene and speciated monoterpenes. Isoprene and monoterpene emissions were found
673 to be highly influenced by anthropogenic sources, with strong correlations to anthropogenic tracers
674 at night across both campaigns. High nocturnal concentrations of pollutants were observed due to a
675 low boundary layer height and stagnant conditions, especially during the post-monsoon period.

676 Isoprene OS markers (OSi) were observed in higher concentrations during the post-monsoon (557 ±
677 423) ng m^{-3} compared to the pre-monsoon campaign (238 ± 118) ng m^{-3}. OSi showed a moderate
678 correlation with inorganic sulfate across both campaigns. However, concentrations levelled off at
679 high sulfate concentrations during the post-monsoon which is consistent with organic coatings
680 limiting uptake of isoprene epoxides. Isoprene NOS species (NOSi) showed nocturnal enhancements
681 across both campaigns, while the highest average concentrations were observed in the morning
682 samples of the post-monsoon campaign. The high morning concentrations are likely due to the
683 oxidation of VOCs by OH radicals from photolytic processes throughout the morning. Monoterpene
684 derived OS (OS_{MT}) and NOS (NOS_{MT}) markers were observed to have nocturnal enhancements in
685 concentrations, in-line with their precursors. NOS_{MT} markers were observed in similar concentrations
686 to those of other megacities. Total quantified SOA contributed on average (2.0 ± 0.9) % and (1.8 ±
687 1.4) % to the total OOA. Considering high OOA concentrations were observed across the two
688 campaigns, the total markers contributed up to a maximum of 4.2 % and 6.6 % across the pre- and
689 post-monsoon respectively. Overall, this work highlights that even small numbers of isoprene and

690 monoterpene derived SOA markers can make significant contributions to OA mass, even in highly
691 polluted megacities.

692

693 Table 1. Molecular formulae, retention times and time weighted means (ng m^{-3}) of
694 organosulfates (OS) and nitrooxy oganosulfates (NOS) from isoprene (i) and monoterpenes
(MT) observed across pre- and post-monsoon campaigns in Delhi.
695

Class	Molecular formula	Pre-	SD	Post-	SD	RT's (min)
OS$_i$	$C_5H_{12}O_7S$	38.79	30.19	17.91	19.87	0.71
	$C_5H_{10}O_5S$	26.16	23.30	53.63	131.19	0.93
	$C_2H_4O_6S$	21.35	18.27	84.65	82.79	0.73
	$C_5H_{10}O_6S$	19.80	13.78	45.87	29.47	0.79
	$C_4H_8O_7S$	19.70	12.48	47.96	39.01	0.73
	$C_3H_6O_5S$	19.50	12.47	35.27	40.15	0.73
	$C_5H_8O_7S$	18.76	11.01	38.75	25.34	0.73
	$C_4H_8O_6S$	16.57	9.77	45.48	37.46	0.74
	$C_5H_{10}O_7S$	11.82	7.04	25.89	18.06	0.73
	$C_3H_6O_6S$	6.64	5.00	38.06	40.30	0.73
	$C_4H_8O_5S$	6.46	4.08	22.44	21.39	0.75
	$C_5H_{10}O_8S$	6.25	5.07	7.00	5.54	0.73
	$C_2H_4O_5S$	5.33	3.37	15.92	13.79	0.73
	$C_2H_6O_5S$	5.23	6.36	24.99	20.38	0.73
	$C_5H_8O_5S$	5.16	2.57	7.87	7.93	0.85
	$C_3H_6O_7S$	3.54	3.49	14.78	11.50	0.75
	$C_5H_{12}O_6S$	2.01	1.23	6.53	4.32	0.74
	$C_3H_8O_6S$	1.90	1.08	12.25	10.82	0.75
	$C_5H_8O_9S$	1.20	1.04	2.12	1.85	0.64
	$C_4H_6O_6S$	1.10	0.76	8.61	15.65	0.74
	$C_5H_{12}O_8S$	0.55	0.43	0.65	0.61	0.75
	Total	237.83		556.64		
NOS$_i$	$C_5H_{10}O_{11}N_2S$	18.65	8.77	11.63	8.09	1.39,1.92,2.85,3.4
	$C_5H_{11}O_9NS$	8.55	5.71	5.93	5.06	0.86
	$C_5H_9O_{10}NS$	3.91	3.46	1.42	1.31	0.94
	$C_5H_{11}O_8NS$	1.52	0.84	1.17	1.20	1.09
	$C_5H_9O_{13}N_3S$	0.002	0.001	0.011	0.009	6.67,7.89,8.06
	Total	32.63		20.15		
OS$_{MT}$	$C_9H_{16}O_6S$	1.10	0.61	1.67	0.88	6.67/7.14/7.5/8.3
	$C_{10}H_{18}O_5S$	0.56	0.63	0.10	0.12	3.39
	$C_{10}H_{16}O_5S$	0.28	0.13	0.77	0.06	4.91/7/9.08/10.9/11.33/11.97/13.26
	$C_{10}H_{20}O_7S$	0.25	0.21	0.27	0.21	4.19
	$C_{10}H_{16}O_7S$	0.23	0.15	0.21	0.13	3.61/11.68
	$C_9H_{16}O_7S$	0.16	0.17	0.22	0.19	4.39/6.77
	$C_{10}H_{18}O_6S$	0.15	0.10	NA	NA	10.27

Atmospheric
Chemistry
and Physics
Discussions
Open Access
EGU

$C_9H_{14}O_6S$	0.15	1.10	0.25	0.14	3.5/5.81
$C_{10}H_{16}O_6S$	0.10	0.06	0.06	0.03	9.33
$C_{10}H_{18}O_8S$	0.02	0.01	0.04	0.24	7.24
$C_8H_{14}O_7S$	0.04	0.03	0.10	0.15	4.46
Total	3.05		3.68		
NOS_{MT} $C_{10}H_{17}NO_7S$	5.96	3.33	13.36	4.98	9.1/10.16/10.67/10.92/11.07/11.36/11.57/12.01/13.28
$C_9H_{15}NO_8S$	1.12	0.51	2.79	1.14	3.5/5.81
$C_{10}H_{17}NO_9S$	0.47	0.19	1.15	0.29	3.93/5.34/6.39/7.89/9.26/10.11/17.94
$C_9H_{15}NO_9S$	0.0216	0.0044	0.22	0.14	2.69/3.46
$C_{10}H_{17}NO_8S$	0.01	0.01	0.07	0.04	5.77
Total	7.59		17.59		

696

697

698

699

700

Table 2. Comparison of $C_{10}H_{17}NO_7S$ concentrations across different locations.
701 Locations and concentrations in bold were quantfified by authentic standards.

702

Location	$C_{10}H_{17}NO_7S$ (ng m^{-3})	Reference
Delhi Pre-monsoon	**5.96**	**This study**
Delhi Post-monsoon	**13.36**	**This study**
Guangzhou summer	7.15	Bryant et al., 2021
Guangzhou winter	11.11	Bryant et al., 2021
Shanghai 15/16	6.21	Wang et al., 2021b
Shanghai 16/17	5.55	Wang et al., 2021b
Beijing	12.00	Wang et al., 2018b
Atlanta	9.00	Hettiyadura et al., 2019
Hong Kong	5.61	Wang et al., 2021a
Guangzhou	12.32	Wang et al., 2021a
Shanghai	16.51	Wang et al., 2021a
Beijing	13.15	Wang et al., 2021a

703

Data availability

705 Data used in this study can be accessed from the CEDA
706 archive: https://catalogue.ceda.ac.uk/uuid/ba27c1c6a03b450e9269f668566658ec (Nemitz et al.,
707 2020).

Author contributions

709 DJB prepared the manuscript with contributions from all authors. DJB, BSN, SJS, SHB, WSD, ARV,
710 JMC, WJFA, BL, EN and JRH provided measurements and data processing of pollutants used in this

711   study. MJN and ARR contributed to scientific discussion. S, RG, BRG, TH and EN assisted with
712   logistics. CNH, JDL, ARR, JFH provided overall guidance to the experimental setup and design.

728   **Competing interests**

729   The authors declare that they have no conflict of interest.

730   **References**

731   Anand, V., Korhale, N., Rathod, A. and Beig, G.: On processes controlling fine particulate matters in
732   four Indian megacities, Environ. Pollut., 254, doi:10.1016/j.envpol.2019.113026, 2019.

733   Anon: Import Surface Meteorological Data from NOAA Integrated Surface Database (ISD) •
734   worldmet, [online] Available from: https://davidcarslaw.github.io/worldmet/index.html (Accessed
735   24 October 2021), n.d.

736   Åsa M. Jonsson, *, Mattias Hallquist, and and Ljungström, E.: Impact of Humidity on the Ozone
737   Initiated Oxidation of Limonene, Δ3-Carene, and α-Pinene, Environ. Sci. Technol., 40(1), 188–194,
738   doi:10.1021/ES051163W, 2005.

739   Atkinson, R. and Arey, J.: Gas-phase tropospheric chemistry of biogenic volatile organic compounds:
740   A review, Atmos. Environ., 37(SUPPL. 2), 197–219, doi:10.1016/S1352-2310(03)00391-1, 2003.

741   Balakrishnan, K., Dey, S., Gupta, T., Dhaliwal, R. S., Brauer, M., Cohen, A. J., Stanaway, J. D., Beig, G.,
742   Joshi, T. K., Aggarwal, A. N., Sabde, Y., Sadhu, H., Frostad, J., Causey, K., Godwin, W., Shukla, D. K.,
743   Kumar, G. A., Varghese, C. M., Muraleedharan, P., Agrawal, A., Anjana, R. M., Bhansali, A., Bhardwaj,
744   D., Burkart, K., Cercy, K., Chakma, J. K., Chowdhury, S., Christopher, D. J., Dutta, E., Furtado, M.,
745   Ghosh, S., Ghoshal, A. G., Glenn, S. D., Guleria, R., Gupta, R., Jeemon, P., Kant, R., Kant, S., Kaur, T.,
746   Koul, P. A., Krish, V., Krishna, B., Larson, S. L., Madhipatla, K., Mahesh, P. A., Mohan, V.,
747   Mukhopadhyay, S., Mutreja, P., Naik, N., Nair, S., Nguyen, G., Odell, C. M., Pandian, J. D.,
748   Prabhakaran, D., Prabhakaran, P., Roy, A., Salvi, S., Sambandam, S., Saraf, D., Sharma, M.,
749   Shrivastava, A., Singh, V., Tandon, N., Thomas, N. J., Torre, A., Xavier, D., Yadav, G., Singh, S.,
750   Shekhar, C., Vos, T., Dandona, R., Reddy, K. S., Lim, S. S., Murray, C. J. L., Venkatesh, S. and Dandona,
751   L.: The impact of air pollution on deaths, disease burden, and life expectancy across the states of
752   India: the Global Burden of Disease Study 2017, Lancet Planet. Heal., 3(1), e26–e39,
753   doi:10.1016/S2542-5196(18)30261-4, 2019.

Atmospheric
Chemistry
and Physics
Discussions
Open Access
EGU

754   Bhandari, S., Gani, S., Patel, K., Wang, D. S., Soni, P., Arub, Z., Habib, G., Apte, J. S. and Hildebrandt
755   Ruiz, L.: Sources and atmospheric dynamics of organic aerosol in New Delhi, India: Insights from
756   receptor modeling, Atmos. Chem. Phys., 20(2), 735–752, doi:10.5194/acp-20-735-2020, 2020.

757   Borbon, A., Fontaine, H., Veillerot, M., Locoge, N., Galloo, J. C. and Guillermo, R.: An investigation
758   into the traffic-related fraction of isoprene at an urban location, Atmos. Environ., 35(22), 3749–3760,
759   doi:10.1016/S1352-2310(01)00170-4, 2001.

760   Brüggemann, M., van Pinxteren, D., Wang, Y., Yu, J. Z. and Herrmann, H.: Quantification of known
761   and unknown terpenoid organosulfates in PM10 using untargeted LC–HRMS/MS: contrasting
762   summertime rural Germany and the North China Plain, Environ. Chem., 16(5), 333,
763   doi:10.1071/EN19089, 2019.

764   Brüggemann, M., Xu, R., Tilgner, A., Kwong, K. C., Mutzel, A., Poon, H. Y., Otto, T., Schaefer, T.,
765   Poulain, L., Chan, M. N. and Herrmann, H.: Organosulfates in Ambient Aerosol: State of Knowledge
766   and Future Research Directions on Formation, Abundance, Fate, and Importance, Environ. Sci.
767   Technol., 54(7), 3767–3782, doi:10.1021/acs.est.9b06751, 2020a.

768   Brüggemann, M., Riva, M., Perrier, S., Poulain, L., George, C. and Herrmann, H.: Overestimation of
769   Monoterpene Organosulfate Abundance in Aerosol Particles by Sampling in the Presence of SO2,
770   Environ. Sci. Technol. Lett., 8, 206–211, doi:10.1021/acs.estlett.0c00814, 2020b.

771   Bryant, D. J., Dixon, W. J., Hopkins, J. R., Dunmore, R. E., Pereira, K. L., Shaw, M., Squires, F. A.,
772   Bannan, T. J., Mehra, A., Worrall, S. D., Bacak, A., Coe, H., Percival, C. J., Whalley, L. K., Heard, D. E.,
773   Slater, E. J., Ouyang, B., Cui, T., Surratt, J. D., Liu, D., Shi, Z., Harrison, R., Sun, Y., Xu, W., Lewis, A. C.,
774   Lee, J. D., Rickard, A. R. and Hamilton, J. F.: Strong anthropogenic control of secondary organic
775   aerosol formation from isoprene in Beijing, Atmos. Chem. Phys., 20(12), 7531–7552,
776   doi:10.5194/acp-20-7531-2020, 2020.

777   Bryant, D. J., Elzein, A., Newland, M., White, E., Swift, S., Watkins, A., Deng, W., Song, W., Wang, S.,
778   Zhang, Y., Wang, X., Rickard, A. R. and Hamilton, J. F.: Importance of Oxidants and Temperature in
779   the Formation of Biogenic Organosulfates and Nitrooxy Organosulfates, ACS Earth Sp. Chem.,
780   acsearthspacechem.1c00204, doi:10.1021/ACSEARTHSPACECHEM.1C00204, 2021.

781   Budisulistiorini, S. H., Li, X., Bairai, S. T., Renfro, J., Liu, Y., Liu, Y. J., McKinney, K. A., Martin, S. T.,
782   McNeill, V. F., Pye, H. O. T., Nenes, A., Neff, M. E., Stone, E. A., Mueller, S., Knote, C., Shaw, S. L.,
783   Zhang, Z., Gold, A. and Surratt, J. D.: Examining the effects of anthropogenic emissions on isoprene-
784   derived secondary organic aerosol formation during the 2013 Southern Oxidant and Aerosol Study
785   (SOAS) at the Look Rock, Tennessee ground site, Atmos. Chem. Phys., 15(15), 8871–8888,
786   doi:10.5194/acp-15-8871-2015, 2015.

787   Cash, J. M., Langford, B., Di Marco, C., Mullinger, N. J., Allan, J., Reyes-Villegas, E., Joshi, R., Heal, M.
788   R., Acton, W. J. F., Hewitt, C. N., Misztal, P. K., Drysdale, W., Mandal, T. K., Gadi, R., Gurjar, B. R. and
789   Nemitz, E.: Seasonal analysis of submicron aerosol in Old Delhi using high-resolution aerosol mass
790   spectrometry: chemical characterisation, source apportionment and new marker identification,
791   Atmos. Chem. Phys., 21(13), 10133–10158, doi:10.5194/ACP-21-10133-2021, 2021a.

792   Cash, J. M., Langford, B., Di Marco, C., Mullinger, N. J., Allan, J., Reyes-Villegas, E., Joshi, R., Heal, M.
793   R., Acton, W. J. F., Hewitt, C. N., Misztal, P. K., Drysdale, W., Mandal, T. K., Shivani, Gadi, R., Gurjar, B.
794   R. and Nemitz, E.: Seasonal analysis of submicron aerosol in Old Delhi using high-resolution aerosol
795   mass spectrometry: Chemical characterisation, source apportionment and new marker
796   identification, Atmos. Chem. Phys., 21(13), 10133–10158, doi:10.5194/ACP-21-10133-2021, 2021b.

797   Chan, M. N., Surratt, J. D., Chan, A. W. H., Schilling, K., Offenberg, J. H., Lewandowski, M., Edney, E.
798   O., Kleindienst, T. E., Jaoui, M., Edgerton, E. S., Tanner, R. L., Shaw, S. L., Zheng, M., Knipping, E. M.
799   and Seinfeld, J. H.: Influence of aerosol acidity on the chemical composition of Secondary Organic

800   Aerosol from &beta;-caryophyllene, Atmos. Chem. Phys. Discuss., 10(11), 29249–29289,
801   doi:10.5194/acpd-10-29249-2010, 2010.

802   Chen, Y., Xu, L., Humphry, T., Hettiyadura, A. P. S., Ovadnevaite, J., Huang, S., Poulain, L., Schroder, J.
803   C., Campuzano-Jost, P., Jimenez, J. L., Herrmann, H., O'Dowd, C., Stone, E. A. and Ng, N. L.: Response
804   of the Aerodyne Aerosol Mass Spectrometer to Inorganic Sulfates and Organosulfur Compounds:
805   Applications in Field and Laboratory Measurements, Environ. Sci. Technol., 53(9), 5176–5186,
806   doi:10.1021/ACS.EST.9B00884/ASSET/IMAGES/MEDIUM/ES-2019-00884R_0003.GIF, 2019.

807   Chen, Y., Zhang, Y., T. Lambe, A., Xu, R., Lei, Z., E. Olson, N., Zhang, Z., Szalkowski, T., Cui, T., Vizuete,
808   W., Gold, A., J. Turpin, B., P Ault, A., Nin Chan, M. and D. Surratt, J.: Heterogeneous Hydroxyl Radical
809   Oxidation of Isoprene Epoxydiol-Derived Methyltetrol Sulfates: Plausible Formation Mechanisms of
810   Previously Unexplained Organosulfates in Ambient Fine Aerosols, Environ. Sci. & Technol. Lett.,
811   0(ja), doi:10.1021/acs.estlett.0c00276, 2020.

812   Cheng, X., Li, H., Zhang, Y., Li, Y., Zhang, W., Wang, X., Bi, F., Zhang, H., Gao, J., Chai, F., Lun, X., Chen,
813   Y. and Lv, J.: Atmospheric isoprene and monoterpenes in a typical urban area of Beijing: Pollution
814   characterization, chemical reactivity and source identification, J. Environ. Sci., 71, 150–167,
815   doi:10.1016/J.JES.2017.12.017, 2018.

816   Chowdhury, Z., Zheng, M., Cass, G. R., Sheesley, R. J., Schauer, J. J., Salmon, L. G. and Russell, A. G.:
817   Source apportionment and characterization of ambient fine particles in Delhi, in Symposium on Air
818   Quality Measurement Methods and Technology 2004, pp. 13–24., 2004.

819   Coggon, M. M., Gilman, J., McDonald, B., Gkatzelis, G., Ortega, J. V., Peischl, J., Aikin, K. C., Warneke,
820   C., Coggon, M. M., Gilman, J., McDonald, B., Gkatzelis, G., Ortega, J. V., Peischl, J., Aikin, K. C. and
821   Warneke, C.: Significant anthropogenic monoterpene emissions from fragrances and other
822   consumer products in New York City., AGUFM, 2018, A32E-08 [online] Available from:
823   https://ui.adsabs.harvard.edu/abs/2018AGUFM.A32E..08C/abstract (Accessed 26 August 2021),
824   2018.

825   Darer, A. I., Cole-Filipiak, N. C., O'Connor, A. E. and Elrod, M. J.: Formation and stability of
826   atmospherically relevant isoprene-derived organosulfates and organonitrates, Environ. Sci. Technol.,
827   45(5), 1895–1902, doi:10.1021/es103797z, 2011.

828   Ding, J., Zhao, P., Su, J., Dong, Q., Du, X. and Zhang, Y.: Aerosol pH and its driving factors in Beijing,
829   Atmos. Chem. Phys., 19(12), 7939–7954, doi:10.5194/ACP-19-7939-2019, 2019.

830   Drozd, G. T., Woo, J. L. and McNeill, V. F.: Self-limited uptake of α-pinene oxide to acidic aerosol: The
831   effects of liquid-liquid phase separation and implications for the formation of secondary organic
832   aerosol and organosulfates from epoxides, Atmos. Chem. Phys., 13(16), 8255–8263,
833   doi:10.5194/acp-13-8255-2013, 2013.

834   Du, Z., He, K., Cheng, Y., Duan, F., Ma, Y., Liu, J., Zhang, X., Zheng, M. and Weber, R.: A yearlong study
835   of water-soluble organic carbon in Beijing I: Sources and its primary vs. secondary nature, Atmos.
836   Environ., 92, 514–521, doi:10.1016/j.atmosenv.2014.04.060, 2014.

837   Eddingsaas, N. C., Loza, C. L., Yee, L. D., Seinfeld, J. H. and Wennberg, P. O.: α-pinene photooxidation
838   under controlled chemical conditions-Part 1: Gas-phase composition in low-and high-NO
839   xenvironments, Atmos. Chem. Phys., 12(14), 6489–6504, doi:10.5194/acp-12-6489-2012, 2012a.

840   Eddingsaas, N. C., Loza, C. L., Yee, L. D., Chan, M., Schilling, K. A., Chhabra, P. S., Seinfeld, J. H. and
841   Wennberg, P. O.: α-pinene photooxidation under controlled chemical conditions-Part 2: SOA yield
842   and composition in low-and high-NO x environments, Atmos. Chem. Phys., 12(16), 7413–7427,
843   doi:10.5194/acp-12-7413-2012, 2012b.

844 Elser, M., Huang, R. J., Wolf, R., Slowik, J. G., Wang, Q., Canonaco, F., Li, G., Bozzetti, C., Daellenbach,
845 K. R., Huang, Y., Zhang, R., Li, Z., Cao, J., Baltensperger, U., El-Haddad, I. and André, P.: New insights
846 into PM2.5 chemical composition and sources in two major cities in China during extreme haze
847 events using aerosol mass spectrometry, Atmos. Chem. Phys., 16(5), 3207–3225, doi:10.5194/ACP-
848 16-3207-2016, 2016.

849 Elzein, A., Stewart, G. J., Swift, S. J., Nelson, B. S., Crilley, L. R., Alam, M. S., Reyes-Villegas, E., Gadi,
850 R., Harrison, R. M., Hamilton, J. F. and Lewis, A. C.: A comparison of PM2.5-bound polycyclic
851 aromatic hydrocarbons in summer Beijing (China) and Delhi (India), Atmos. Chem. Phys., 20(22),
852 14303–14319, doi:10.5194/ACP-20-14303-2020, 2020.

853 Galloway, M. M., Chhabra, P. S., Chan, A. W. H., Surratt, J. D., Flagan, R. C., Seinfeld, J. H. and
854 Keutsch, F. N.: Glyoxal uptake on ammonium sulphate seed aerosol: Reaction products and
855 reversibility of uptake under dark and irradiated conditions, Atmos. Chem. Phys., 9(10), 3331–3345,
856 doi:10.5194/acp-9-3331-2009, 2009.

857 Gani, S., Bhandari, S., Seraj, S., Wang, D. S., Patel, K., Soni, P., Arub, Z., Habib, G., Hildebrandt Ruiz, L.
858 and Apte, J. S.: Submicron aerosol composition in the world's most polluted megacity: the Delhi
859 Aerosol Supersite study, Atmos. Chem. Phys., 19(10), 6843–6859, doi:10.5194/acp-19-6843-2019,
860 2019.

861 Gaston, C. J., Riedel, T. P., Zhang, Z., Gold, A., Surratt, J. D. and Thornton, J. A.: Reactive Uptake of an
862 Isoprene-Derived Epoxydiol to Submicron Aerosol Particles, Environ. Sci. Technol., 48(19), 11178–
863 11186, doi:10.1021/es5034266, 2014.

864 Gkatzelis, G. I., Coggon, M. M., McDonald, B. C., Peischl, J., Gilman, J. B., Aikin, K. C., Robinson, M. A.,
865 Canonaco, F., Prevot, A. S. H., Trainer, M. and Warneke, C.: Observations Confirm that Volatile
866 Chemical Products Are a Major Source of Petrochemical Emissions in U.S. Cities, Environ. Sci.
867 Technol., 55(8), 4332–4343, doi:10.1021/ACS.EST.0C05471/SUPPL_FILE/ES0C05471_SI_001.PDF,
868 2021.

869 Glasius, M., Bering, M. S., Yee, L. D., de Sá, S. S., Isaacman-VanWertz, G., Wernis, R. A., Barbosa, H.
870 M. J., Alexander, M. L., Palm, B. B., Hu, W., Campuzano-Jost, P., Day, D. A., Jimenez, J. L., Shrivastava,
871 M., Martin, S. T. and Goldstein, A. H.: Organosulfates in aerosols downwind of an urban region in
872 central Amazon, Environ. Sci. Process. Impacts, 20(11), 1546–1558, doi:10.1039/C8EM00413G, 2018.

873 Guenther, A. B., Jiang, X., Heald, C. L., Sakulyanontvittaya, T., Duhl, T., Emmons, L. K. and Wang, X.:
874 The Model of Emissions of Gases and Aerosols from Nature version 2.1 (MEGAN2.1): an extended
875 and updated framework for modeling biogenic emissions, Geosci. Model Dev., 5(6), 1471–1492,
876 doi:10.5194/gmd-5-1471-2012, 2012.

877 Hallquist, M., Wenger, J. C., Baltensperger, U., Rudich, Y., Simpson, D., Claeys, M., Dommen, J.,
878 Donahue, N. M., George, C., Goldstein, A. H., Hamilton, J. F., Herrmann, H., Hoffmann, T., Iinuma, Y.,
879 Jang, M., Jenkin, M. E., Jimenez, J. L., Kiendler-Scharr, A., Maenhaut, W., McFiggans, G., Mentel, T. F.,
880 Monod, A., Prévôt, A. S. H., Seinfeld, J. H., Surratt, J. D., Szmigielski, R. and Wildt, J.: The formation,
881 properties and impact of secondary organic aerosol: current and emerging issues, Atmos. Chem.
882 Phys., 9(14), 5155–5236, doi:10.5194/acp-9-5155-2009, 2009.

883 Hama, S. M. L., Kumar, P., Harrison, R. M., Bloss, W. J., Khare, M., Mishra, S., Namdeo, A., Sokhi, R.,
884 Goodman, P. and Sharma, C.: Four-year assessment of ambient particulate matter and trace gases in
885 the Delhi-NCR region of India, Sustain. Cities Soc., 54, doi:10.1016/j.scs.2019.102003, 2020.

886 Hamilton, J. F., Bryant, D. J., Edwards, P. M., Ouyang, B., Bannan, T. J., Mehra, A., Mayhew, A. W.,
887 Hopkins, J. R., Dunmore, R. E., Squires, F. A., Lee, J. D., Newland, M. J., Worrall, S. D., Bacak, A., Coe,
888 H., Whalley, L. K., Heard, D. E., Slater, E. J., Jones, R. L., Cui, T., Surratt, J. D., Reeves, C. E., Mills, G. P.,
889 Grimmond, S., Sun, Y., Xu, W., Shi, Z. and Rickard, A. R.: Key Role of NO3 Radicals in the Production

Atmospheric
Chemistry
and Physics
Discussions

890   of Isoprene Nitrates and Nitrooxyorganosulfates in Beijing, Environ. Sci. Technol., 55(2), 842–853,
891   doi:10.1021/acs.est.0c05689, 2021.

892   Hatch, L. E., Jen, C. N., Kreisberg, N. M., Selimovic, V., Yokelson, R. J., Stamatis, C., York, R. A., Foster,
893   D., Stephens, S. L., Goldstein, A. H. and Barsanti, K. C.: Highly Speciated Measurements of Terpenoids
894   Emitted from Laboratory and Mixed-Conifer Forest Prescribed Fires, Environ. Sci. Technol., 53(16),
895   9418–9428, doi:10.1021/ACS.EST.9B02612, 2019.

896   Hettiyadura, A. P. S., Al-Naiema, I. M., Hughes, D. D., Fang, T. and Stone, E. A.: Organosulfates in
897   Atlanta, Georgia: anthropogenic influences on biogenic secondary organic aerosol formation, Atmos.
898   Chem. Phys., 19(5), 3191–3206, doi:10.5194/acp-19-3191-2019, 2019.

899   Hoffmann, T., Odum, J. R., Bowman, F., Collins, D., Klockow, D., Flagan, R. C. and Seinfeld, J. H.:
900   Formation of organic aerosols from the oxidation of biogenic hydrocarbons, J. Atmos. Chem., 26(2),
901   189–222, doi:10.1023/A:1005734301837, 1997.

902   Hoyle, C. R., Boy, M., Donahue, N. M., Fry, J. L., Glasius, M., Guenther, A., Hallar, A. G., Huff Hartz, K.,
903   Petters, M. D., Petäjä, T., Rosenoern, T. and Sullivan, A. P.: A review of the anthropogenic influence
904   on biogenic secondary organic aerosol, Atmos. Chem. Phys., 11(1), 321–343, doi:10.5194/acp-11-
905   321-2011, 2011.

906   Hsieh, H.-C., Ou-Yang, C.-F. and Wang, J.-L.: Revelation of Coupling Biogenic with Anthropogenic
907   Isoprene by Highly Time-Resolved Observations, Aerosol Air Qual. Res., 17(3), 721–729,
908   doi:10.4209/AAQR.2016.04.0133, 2017.

909   Hu, W., Hu, M., Hu, W., Jimenez, J. L., Yuan, B., Chen, W., Wang, M., Wu, Y., Chen, C., Wang, Z., Peng,
910   J., Zeng, L. and Shao, M.: Chemical composition, sources, and aging process of submicron aerosols in
911   Beijing: Contrast between summer and winter, J. Geophys. Res. Atmos., 121(4), 1955–1977,
912   doi:10.1002/2015JD024020, 2016.

913   Huang, Z., Zhang, Y., Yan, Q., Zhang, Z. and Wang, X.: Real-time monitoring of respiratory absorption
914   factors of volatile organic compounds in ambient air by proton transfer reaction time-of-flight mass
915   spectrometry, J. Hazard. Mater., 320, 547–555, doi:10.1016/J.JHAZMAT.2016.08.064, 2016.

916   Iinuma, Y., Müller, C., Berndt, T., Böge, O., Claeys, M. and Herrmann, H.: Evidence for the existence
917   of organosulfates from β-pinene ozonolysis in ambient secondary organic aerosol, Environ. Sci.
918   Technol., 41(19), 6678–6683, doi:10.1021/es070938t, 2007.

919   Javed, M., Bashir, M. and Zaineb, S.: Analysis of daily and seasonal variation of fine particulate
920   matter (PM2.5) for five cities of China, Environ. Dev. Sustain., 1–29, doi:10.1007/s10668-020-01159-
921   1, 2021.

922   Kanawade, V. P., Srivastava, A. K., Ram, K., Asmi, E., Vakkari, V., Soni, V. K., Varaprasad, V. and
923   Sarangi, C.: What caused severe air pollution episode of November 2016 in New Delhi?, Atmos.
924   Environ., 222, doi:10.1016/j.atmosenv.2019.117125, 2020.

925   Kashyap, P., Kumar, A., Kumar, R. P. and Kumar, K.: Biogenic and anthropogenic isoprene emissions
926   in the subtropical urban atmosphere of Delhi, Atmos. Pollut. Res., 10(5), 1691–1698,
927   doi:10.1016/j.apr.2019.07.004, 2019.

928   Khan, M. A. H., Schlich, B.-L., Jenkin, M. E., Shallcross, B. M. A., Moseley, K., Walker, C., Morris, W. C.,
929   Derwent, R. G., Percival, C. J. and Shallcross, D. E.: A Two-Decade Anthropogenic and Biogenic
930   Isoprene Emissions Study in a London Urban Background and a London Urban Traffic Site, Atmos.
931   2018, Vol. 9, Page 387, 9(10), 387, doi:10.3390/ATMOS9100387, 2018a.

932   Khan, M. A. H., Schlich, B. L., Jenkin, M. E., Shallcross, B. M. A., Moseley, K., Walker, C., Morris, W. C.,
933   Derwent, R. G., Percival, C. J. and Shallcross, D. E.: A Two-Decade Anthropogenic and Biogenic

934   Isoprene Emissions Study in a London Urban Background and a London Urban Traffic Site, Atmos.
935   2018, Vol. 9, Page 387, 9(10), 387, doi:10.3390/ATMOS9100387, 2018b.

936   Kirillova, E. N., Sheesley, R. J., Andersson, A. and Gustafsson, Ö.: Natural abundance 13C and 14C
937   analysis of water-soluble organic carbon in atmospheric aerosols, Anal. Chem., 82(19), 7973–7978,
938   doi:10.1021/ac1014436, 2010.

939   Kirillova, E. N., Andersson, A., Sheesley, R. J., Kruså, M., Praveen, P. S., Budhavant, K., Safai, P. D.,
940   Rao, P. S. P. and Gustafsson, Ö.: ^{13}C- and ^{14}C-based study of sources and atmospheric processing of
941   water-soluble organic carbon (WSOC) in South Asian aerosols, J. Geophys. Res. Atmos., 118(2), 614–
942   626, doi:10.1002/jgrd.50130, 2013.

943   Kirillova, E. N., Andersson, A., Tiwari, S., Srivastava, A. K., Bisht, D. S. and Gustafsson, Ö.: Water-
944   soluble organic carbon aerosols during a full New Delhi winter: Isotope-based source apportionment
945   and optical properties, J. Geophys. Res. Atmos., 119(6), 3476–3485, doi:10.1002/2013JD020041,
946   2014.

947   Klein, F., Farren, N. J., Bozzetti, C., Daellenbach, K. R., Kilic, D., Kumar, N. K., Pieber, S. M., Slowik, J.
948   G., Tuthill, R. N., Hamilton, J. F., Baltensperger, U., Prévôt, A. S. H. and El Haddad, I.: Indoor terpene
949   emissions from cooking with herbs and pepper and their secondary organic aerosol production
950   potential, Sci. Reports 2016 61, 6(1), 1–7, doi:10.1038/srep36623, 2016.

951   Kleindienst, T. E., Edney, E. O., Lewandowski, M., Offenberg, J. H. and Jaoui, M.: Secondary Organic
952   Carbon and Aerosol Yields from the Irradiations of Isoprene and α-Pinene in the Presence of NO $_x$
953   and SO $_2$, Environ. Sci. Technol., 40(12), 3807–3812, doi:10.1021/es052446r, 2006.

954   Kourtchev, I., Godoi, R. H. M., Connors, S., Levine, J. G., Archibald, A. T., Godoi, A. F. L., Paralovo, S.
955   L., Barbosa, C. G. G., Souza, R. A. F., Manzi, A. O., Seco, R., Sjostedt, S., Park, J. H., Guenther, A., Kim,
956   S., Smith, J., Martin, S. T. and Kalberer, M.: Molecular composition of organic aerosols in central
957   Amazonia: An ultra-high-resolution mass spectrometry study, Atmos. Chem. Phys., 16(18), 11899–
958   11913, doi:10.5194/acp-16-11899-2016, 2016.

959   Kristensen, K., Enggrob, K. L., King, S. M., Worton, D. R., Platt, S. M., Mortensen, R., Rosenoern, T.,
960   Surratt, J. D., Bilde, M., Goldstein, A. H. and Glasius, M.: Formation and occurrence of dimer esters of
961   pinene oxidation products in atmospheric aerosols, Atmos. Chem. Phys., 13(7), 3763–3776,
962   doi:10.5194/acp-13-3763-2013, 2013.

963   Kumar, P., Kumar, S. and Yadav, S.: Seasonal variations in size distribution, water-soluble ions, and
964   carbon content of size-segregated aerosols over New Delhi, Environ. Sci. Pollut. Res., 25(6), 6061–
965   6078, doi:10.1007/S11356-017-0954-6, 2018.

966   Landrigan, P. J., Fuller, R., Acosta, N. J. R., Adeyi, O., Arnold, R., Basu, N. (Nil), Baldé, A. B., Bertollini,
967   R., Bose-O'Reilly, S., Boufford, J. I., Breysse, P. N., Chiles, T., Mahidol, C., Coll-Seck, A. M., Cropper, M.
968   L., Fobil, J., Fuster, V., Greenstone, M., Haines, A., Hanrahan, D., Hunter, D., Khare, M., Krupnick, A.,
969   Lanphear, B., Lohani, B., Martin, K., Mathiasen, K. V., McTeer, M. A., Murray, C. J. L., Ndahimananjara,
970   J. D., Perera, F., Potočnik, J., Preker, A. S., Ramesh, J., Rockström, J., Salinas, C., Samson, L. D.,
971   Sandilya, K., Sly, P. D., Smith, K. R., Steiner, A., Stewart, R. B., Suk, W. A., van Schayck, O. C. P.,
972   Yadama, G. N., Yumkella, K. and Zhong, M.: The Lancet Commission on pollution and health, Lancet,
973   391(10119), 462–512, doi:10.1016/S0140-6736(17)32345-0, 2018.

974   Lanz, V. A., Prévôt, A. S. H., Alfarra, M. R., Weimer, S., Mohr, C., Decarlo, P. F., Gianini, M. F. D.,
975   Hueglin, C., Schneider, J., Favez, O., D'Anna, B., George, C. and Baltensperger, U.: Characterization of
976   aerosol chemical composition with aerosol mass spectrometry in Central Europe: An overview,
977   Atmos. Chem. Phys., 10(21), 10453–10471, doi:10.5194/ACP-10-10453-2010, 2010.

978   Lee, B. H., Mohr, C., Lopez-Hilfiker, F. D., Lutz, A., Hallquist, M., Lee, L., Romer, P., Cohen, R. C., Iyer,

979 S., Kurtén, T., Hu, W., Day, D. A., Campuzano-Jost, P., Jimenez, J. L., Xu, L., Ng, N. L., Guo, H., Weber,
980 R. J., Wild, R. J., Brown, S. S., Koss, A., de Gouw, J., Olson, K., Goldstein, A. H., Seco, R., Kim, S.,
981 McAvey, K., Shepson, P. B., Starn, T., Baumann, K., Edgerton, E. S., Liu, J., Shilling, J. E., Miller, D. O.,
982 Brune, W., Schobesberger, S., D'Ambro, E. L. and Thornton, J. A.: Highly functionalized organic
983 nitrates in the southeast United States: Contribution to secondary organic aerosol and reactive
984 nitrogen budgets., Proc. Natl. Acad. Sci. U. S. A., 113(6), 1516–21, doi:10.1073/pnas.1508108113,
985 2016.

986 Liao, J., Froyd, K. D., Murphy, D. M., Keutsch, F. N., Yu, G., Wennberg, P. O., St. Clair, J. M., Crounse,
987 J. D., Wisthaler, A., Mikoviny, T., Jimenez, J. L., Campuzano-Jost, P., Day, D. A., Hu, W., Ryerson, T. B.,
988 Pollack, I. B., Peischl, J., Anderson, B. E., Ziemba, L. D., Blake, D. R., Meinardi, S. and Diskin, G.:
989 Airborne measurements of organosulfates over the continental U.S., J. Geophys. Res., 120(7), 2990–
990 3005, doi:10.1002/2014JD022378, 2015.

991 Lin, Y. H., Zhang, Z., Docherty, K. S., Zhang, H., Budisulistiorini, S. H., Rubitschun, C. L., Shaw, S. L.,
992 Knipping, E. M., Edgerton, E. S., Kleindienst, T. E., Gold, A. and Surratt, J. D.: Isoprene epoxydiols as
993 precursors to secondary organic aerosol formation: Acid-catalyzed reactive uptake studies with
994 authentic compounds, Environ. Sci. Technol., 46(1), 250–258, doi:10.1021/es202554c, 2012.

995 Lin, Y. H., Zhang, H., Pye, H. O. T., Zhang, Z., Marth, W. J., Park, S., Arashiro, M., Cui, T.,
996 Budisulistiorini, S. H., Sexton, K. G., Vizuete, W., Xie, Y., Luecken, D. J., Piletic, I. R., Edney, E. O.,
997 Bartolotti, L. J., Gold, A. and Surratt, J. D.: Epoxide as a precursor to secondary organic aerosol
998 formation from isoprene photooxidation in the presence of nitrogen oxides, Proc. Natl. Acad. Sci. U.
999 S. A., 110(17), 6718–6723, doi:10.1073/pnas.1221150110, 2013a.

1000 Lin, Y. H., Knipping, E. M., Edgerton, E. S., Shaw, S. L. and Surratt, J. D.: Investigating the influences of
1001 SO2 and NH3 levels on isoprene-derived secondary organic aerosol formation using conditional
1002 sampling approaches, Atmos. Chem. Phys., 13(16), 8457–8470, doi:10.5194/ACP-13-8457-2013,
1003 2013b.

1004 Lin, Y. H., Budisulistiorini, S. H., Chu, K., Siejack, R. A., Zhang, H., Riva, M., Zhang, Z., Gold, A.,
1005 Kautzman, K. E. and Surratt, J. D.: Light-absorbing oligomer formation in secondary organic aerosol
1006 from reactive uptake of isoprene epoxydiols, Environ. Sci. Technol., 48(20), 12012–12021,
1007 doi:10.1021/es503142b, 2014.

1008 Mishra, A. K. and Sinha, V.: Emission drivers and variability of ambient isoprene, formaldehyde and
1009 acetaldehyde in north-west India during monsoon season, Environ. Pollut., 267, 115538,
1010 doi:10.1016/J.ENVPOL.2020.115538, 2020.

1011 Miyazaki, Y., Aggarwal, S. G., Singh, K., Gupta, P. K. and Kawamura, K.: Dicarboxylic acids and water-
1012 soluble organic carbon in aerosols in New Delhi, India, in winter: Characteristics and formation
1013 processes, J. Geophys. Res. Atmos., 114(19), doi:10.1029/2009JD011790, 2009.

1014 Morales, A. C., Jayarathne, T., Slade, J. H., Laskin, A. and Shepson, P. B.: The production and
1015 hydrolysis of organic nitrates from OH radical oxidation of β-ocimene, Atmos. Chem. Phys., 21(1),
1016 129–145, doi:10.5194/ACP-21-129-2021, 2021.

1017 Mutzel, A., Rodigast, M., Iinuma, Y., Böge, O. and Herrmann, H.: Monoterpene SOA - Contribution of
1018 first-generation oxidation products to formation and chemical composition, Atmos. Environ., 130,
1019 136–144, doi:10.1016/j.atmosenv.2015.10.080, 2016.

1020 Nagar, P. K., Singh, D., Sharma, M., Kumar, A., Aneja, V. P., George, M. P., Agarwal, N. and Shukla, S.
1021 P.: Characterization of PM2.5 in Delhi: role and impact of secondary aerosol, burning of biomass, and
1022 municipal solid waste and crustal matter, Environ. Sci. Pollut. Res., 24(32), 25179–25189,
1023 doi:10.1007/s11356-017-0171-3, 2017.

1024   Nelson, B., Stewart, G., Drysdale, W., Newland, M., Vaughan, A., Dunmore, R., Edwards, P., Lewis, A.,
1025   Hamilton, J., Acton, W. J. F., Hewitt, C. N., Crilley, L., Alam, M., Şahin, Ü., Beddows, D., Bloss, W.,
1026   Slater, E., Whalley, L., Heard, D., Cash, J., Langford, B., Nemitz, E., Sommariva, R., Cox, S., Gadi, R.,
1027   Gurjar, B., Hopkins, J., Rickard, A. and Lee, J.: In situ Ozone Production is highly sensitive to Volatile
1028   Organic Compounds in the Indian Megacity of Delhi, Atmos. Chem. Phys. Discuss., 1–36,
1029   doi:10.5194/ACP-2021-278, 2021.

1030   Nestorowicz, K., Jaoui, M., Rudzinski, K. J., Lewandowski, M., Kleindienst, T. E., Spólnik, G.,
1031   Danikiewicz, W. and Szmigielski, R.: Chemical composition of isoprene SOA under acidic and non-
1032   acidic conditions: effect of relative humidity, Atmos. Chem. Phys., 18(24), 18101–18121,
1033   doi:10.5194/acp-18-18101-2018, 2018.

1034   Newland, M. J., Bryant, D. J., Dunmore, R. E., Bannan, T. J., Joe, W., Langford, B., Hopkins, J. R.,
1035   Squires, F. A., Dixon, W., Drysdale, W. S., Ivatt, P. D., Evans, M. J., Edwards, P. M., Whalley, L. K.,
1036   Heard, D. E., Slater, E. J., Woodward-Massey, R., Ye, C., Mehra, A., Worrall, S. D., Bacak, A., Coe, H.,
1037   Percival, C. J., Nicholas Hewitt, C., Lee, J. D., Cui, T., Surratt, J. D., Wang, X., Lewis, A. C., Rickard, A. R.
1038   and Hamilton, J. F.: Low-NO atmospheric oxidation pathways in a polluted megacity, Atmos. Chem.
1039   Phys., 21(3), 1613–1625, doi:10.5194/acp-21-1613-2021, 2021.

1040   Ng, N. L., Kwan, A. J., Surratt, J. D., Chan, A. W. H., Chhabra, P. S., Sorooshian, A., Pye, H. O. T.,
1041   Crounse, J. D., Wennberg, P. O., Flagan, R. C. and Seinfeld, J. H.: Secondary organic aerosol (SOA)
1042   formation from reaction of isoprene with nitrate radicals (NO3), Atmos. Chem. Phys., 8(14), 4117–
1043   4140, doi:10.5194/acp-8-4117-2008, 2008.

1044   Ng, N. L., Brown, S. S., Archibald, A. T., Atlas, E., Cohen, R. C., Crowley, J. N., Day, D. A., Donahue, N.
1045   M., Fry, J. L., Fuchs, H., Griffin, R. J., Guzman, M. I., Herrmann, H., Hodzic, A., Iinuma, Y., Jimenez, J.
1046   L., Kiendler-Scharr, A., Lee, B. H., Luecken, D. J., Mao, J., McLaren, R., Mutzel, A., Osthoff, H. D.,
1047   Ouyang, B., Picquet-Varrault, B., Platt, U., Pye, H. O. T., Rudich, Y., Schwantes, R. H., Shiraiwa, M.,
1048   Stutz, J., Thornton, J. A., Tilgner, A., Williams, B. J. and Zaveri, R. A.: Nitrate radicals and biogenic
1049   volatile organic compounds: oxidation, mechanisms, and organic aerosol, Atmos. Chem. Phys., 17(3),
1050   2103–2162, doi:10.5194/acp-17-2103-2017, 2017.

1051   Nguyen, T. B., Bateman, A. P., Bones, D. L., Nizkorodov, S. A., Laskin, J. and Laskin, A.: High-resolution
1052   mass spectrometry analysis of secondary organic aerosol generated by ozonolysis of isoprene,
1053   Atmos. Environ., 44(8), 1032–1042, doi:10.1016/J.ATMOSENV.2009.12.019, 2010.

1054   Nguyen, T. B., Bates, K. H., Crounse, J. D., Schwantes, R. H., Zhang, X., Kjaergaard, H. G., Surratt, J. D.,
1055   Lin, P., Laskin, A., Seinfeld, J. H. and Wennberg, P. O.: Mechanism of the hydroxyl radical oxidation of
1056   methacryloyl peroxynitrate (MPAN) and its pathway toward secondary organic aerosol formation in
1057   the atmosphere, Phys. Chem. Chem. Phys., 17(27), 17914–17926, doi:10.1039/c5cp02001h, 2015.

1058   None, S., R, G., SK, S. and TK, M.: Seasonal variation, source apportionment and source attributed
1059   health risk of fine carbonaceous aerosols over National Capital Region, India, Chemosphere, 237,
1060   doi:10.1016/J.CHEMOSPHERE.2019.124500, 2019.

1061   Panopoulou, A., Liakakou, E., Sauvage, S., Gros, V., Locoge, N., Stavroulas, I., Bonsang, B.,
1062   Gerasopoulos, E. and Mihalopoulos, N.: Yearlong measurements of monoterpenes and isoprene in a
1063   Mediterranean city (Athens): Natural vs anthropogenic origin, Atmos. Environ., 243, 117803,
1064   doi:10.1016/J.ATMOSENV.2020.117803, 2020.

1065   Panopoulou, A., Liakakou, E., Sauvage, S., Gros, V., Locoge, N., Bonsang, B., Salameh, T.,
1066   Gerasopoulos, E. and Mihalopoulos, N.: Variability and sources of non-methane hydrocarbons at a
1067   Mediterranean urban atmosphere: The role of biomass burning and traffic emissions, Sci. Total
1068   Environ., 800, 149389, doi:10.1016/J.SCITOTENV.2021.149389, 2021.

1069   Passananti, M., Kong, L., Shang, J., Dupart, Y., Perrier, S., Chen, J., Donaldson, D. J. and George, C.:

1070   Organosulfate Formation through the Heterogeneous Reaction of Sulfur Dioxide with Unsaturated
1071   Fatty Acids and Long-Chain Alkenes, Angew. Chemie - Int. Ed., 55(35), 10336–10339,
1072   doi:10.1002/anie.201605266, 2016.

1073   Paulot, F., Crounse, J. D., Kjaergaard, H. G., Kurten, A., St. Clair, J. M., Seinfeld, J. H. and Wennberg, P.
1074   O.: Unexpected Epoxide Formation in the Gas-Phase Photooxidation of Isoprene, Science (80-.).,
1075   325(5941), 730–733, doi:10.1126/science.1172910, 2009.

1076   Rattanavaraha, W., Chu, K., Budisulistiorini, S. H., Riva, M., Lin, Y.-H., Edgerton, E. S., Baumann, K.,
1077   Shaw, S. L., Guo, H., King, L., Weber, R. J., Neff, M. E., Stone, E. A., Offenberg, J. H., Zhang, Z., Gold, A.
1078   and Surratt, J. D.: Assessing the impact of anthropogenic pollution on isoprene-derived secondary
1079   organic aerosol formation in PM&lt;sub&gt;2.5&lt;/sub&gt; collected from the
1080   Birmingham, Alabama, ground site during the 2013 Southern Oxidant and Aerosol Study, Atmos.
1081   Chem. Phys., 16(8), 4897–4914, doi:10.5194/acp-16-4897-2016, 2016a.

1082   Rattanavaraha, W., Chu, K., Budisulistiorini, S. H., Riva, M., Lin, Y. H., Edgerton, E. S., Baumann, K.,
1083   Shaw, S. L., Guo, H., King, L., Weber, R. J., Neff, M. E., Stone, E. A., Offenberg, J. H., Zhang, Z., Gold, A.
1084   and Surratt, J. D.: Assessing the impact of anthropogenic pollution on isoprene-derived secondary
1085   organic aerosol formation in PM2.5 collected from the Birmingham, Alabama, ground site during the
1086   2013 Southern Oxidant and Aerosol Study, Atmos. Chem. Phys., 16(8), 4897–4914, doi:10.5194/acp-
1087   16-4897-2016, 2016b.

1088   Reyes-Villegas, E., Panda, U., Darbyshire, E., Cash, J. M., Joshi, R., Langford, B., Di Marco, C. F.,
1089   Mullinger, N. J., Alam, M. S., Crilley, L. R., Rooney, D. J., Acton, W. J. F., Drysdale, W., Nemitz, E.,
1090   Flynn, M., Voliotis, A., McFiggans, G., Coe, H., Lee, J., Hewitt, C. N., Heal, M. R., Gunthe, S. S., Mandal,
1091   T. K., Gurjar, B. R., Shivani, Gadi, R., Singh, S., Soni, V. and Allan, J. D.: PM1 composition and source
1092   apportionment at two sites in Delhi, India, across multiple seasons, Atmos. Chem. Phys., 21(15),
1093   11655–11667, doi:10.5194/ACP-21-11655-2021, 2021.

1094   Riva, M., Da Silva Barbosa, T., Lin, Y.-H., Stone, E. A., Gold, A. and Surratt, J. D.: Chemical
1095   characterization of organosulfates in secondary organic aerosol derived from the photooxidation of
1096   alkanes, Atmos. Chem. Phys., 16(17), 11001–11018, doi:10.5194/acp-16-11001-2016, 2016a.

1097   Riva, M., Budisulistiorini, S. H., Zhang, Z. and Gold, A.: Chemical characterization of secondary
1098   organic aerosol constituents from isoprene ozonolysis in the presence of acidic aerosol, Atmos.
1099   Environ., 130, 5–13, doi:10.1016/J.ATMOSENV.2015.06.027, 2016b.

1100   Riva, M., Bell, D. M., Hansen, A. M. K., Drozd, G. T., Zhang, Z., Gold, A., Imre, D., Surratt, J. D., Glasius,
1101   M. and Zelenyuk, A.: Effect of Organic Coatings, Humidity and Aerosol Acidity on Multiphase
1102   Chemistry of Isoprene Epoxydiols, Environ. Sci. Technol., 50(11), 5580–5588,
1103   doi:10.1021/acs.est.5b06050, 2016c.

1104   Riva, M., Chen, Y., Zhang, Y., Lei, Z., Olson, N. E., Boyer, H. C., Narayan, S., Yee, L. D., Green, H. S., Cui,
1105   T., Zhang, Z., Baumann, K., Fort, M., Edgerton, E., Budisulistiorini, S. H., Rose, C. A., Ribeiro, I. O., e
1106   Oliveira, R. L., dos Santos, E. O., Machado, C. M. D., Szopa, S., Zhao, Y., Alves, E. G., de Sá, S. S., Hu,
1107   W., Knipping, E. M., Shaw, S. L., Duvoisin Junior, S., de Souza, R. A. F., Palm, B. B., Jimenez, J.-L.,
1108   Glasius, M., Goldstein, A. H., Pye, H. O. T., Gold, A., Turpin, B. J., Vizuete, W., Martin, S. T., Thornton,
1109   J. A., Dutcher, C. S., Ault, A. P. and Surratt, J. D.: Increasing Isoprene Epoxydiol-to-Inorganic Sulfate
1110   Aerosol Ratio Results in Extensive Conversion of Inorganic Sulfate to Organosulfur Forms:
1111   Implications for Aerosol Physicochemical Properties, Environ. Sci. Technol., acs.est.9b01019,
1112   doi:10.1021/acs.est.9b01019, 2019.

1113   Saha, D., Soni, K., Mohanan, M. N. and Singh, M.: Long-term trend of ventilation coefficient over
1114   Delhi and its potential impacts on air quality, Remote Sens. Appl. Soc. Environ., 15, 100234,
1115   doi:10.1016/J.RSASE.2019.05.003, 2019.

1116   Sahu, L. K. and Saxena, P.: High time and mass resolved PTR-TOF-MS measurements of VOCs at an
1117   urban site of India during winter: Role of anthropogenic, biomass burning, biogenic and
1118   photochemical sources, Atmos. Res., 164–165, 84–94, doi:10.1016/J.ATMOSRES.2015.04.021, 2015.

1119   Sahu, L. K., Tripathi, N. and Yadav, R.: Contribution of biogenic and photochemical sources to
1120   ambient VOCs during winter to summer transition at a semi-arid urban site in India, Environ. Pollut.,
1121   229, 595–606, doi:10.1016/J.ENVPOL.2017.06.091, 2017.

1122   Sawlani, R., Agnihotri, R., Sharma, C., Patra, P. K., Dimri, A. P., Ram, K. and Verma, R. L.: The severe
1123   Delhi SMOG of 2016: A case of delayed crop residue burning, coincident firecracker emissions, and
1124   atypical meteorology, Atmos. Pollut. Res., 10(3), 868–879, doi:10.1016/j.apr.2018.12.015, 2019.

1125   Schindelka, J., Iinuma, Y., Hoffmann, D. and Herrmann, H.: Sulfate radical-initiated formation of
1126   isoprene-derived organosulfates in atmospheric aerosols, Faraday Discuss., 165(0), 237–259,
1127   doi:10.1039/c3fd00042g, 2013.

1128   Schnell, J. L., Naik, V., Horowitz, L. W., Paulot, F., Mao, J., Ginoux, P., Zhao, M. and Ram, K.: Exploring
1129   the relationship between surface PM $_{2.5}$ and meteorology in Northern India, Atmos. Chem. Phys.,
1130   18(14), 10157–10175, doi:10.5194/acp-18-10157-2018, 2018.

1131   Sharma, S. K. and Mandal, T. K.: Chemical composition of fine mode particulate matter (PM2.5) in an
1132   urban area of Delhi, India and its source apportionment, Urban Clim., 21, 106–122,
1133   doi:10.1016/j.uclim.2017.05.009, 2017.

1134   Sheesley, R. J., Kirillova, E., Andersson, A., Krusa, M., Praveen, P. S., Budhavant, K., Safai, P. D., Rao,
1135   P. S. P. and Gustafsson, O.: Year-round radiocarbon-based source apportionment of carbonaceous
1136   aerosols at two background sites in South Asia, J. Geophys. Res. Atmos., 117(10),
1137   doi:10.1029/2011JD017161, 2012.

1138   Simon, M., Dada, L., Heinritzi, M., Scholz, W., Stolzenburg, D., Fischer, L., Wagner, A., Kürten, A.,
1139   Rörup, B., He, X.-C., Almeida, J., Baalbaki, R., Baccarini, A., Bauer, P., Beck, L., Bergen, A., Bianchi, F.,
1140   Bräkling, S., Brilke, S., Caudillo, L., Chen, D., Chu, B., Dias, A., Draper, D., Duplissy, J., El Haddad, I.,
1141   Finkenzeller, H., Frege, C., Gonzalez-Carracedo, L., Gordon, H., Granzin, M., Hakala, J., Hofbauer, V.,
1142   Hoyle, C., Kim, C., Kong, W., Lamkaddam, H., Lee, C., Lehtipalo, K., Leiminger, M., Mai, H., Manninen,
1143   H., Marie, G., Marten, R., Mentler, B., Molteni, U., Nichman, L., Nie, W., Ojdanic, A., Onnela, A.,
1144   Partoll, E., Petäjä, T., Pfeifer, J., Philippov, M., Quéléver, L., Ranjithkumar, A., Rissanen, M.,
1145   Schallhart, S., Schobesberger, S., Schuchmann, S., Shen, J., Sipilä, M., Steiner, G., Stozhkov, Y.,
1146   Tauber, C., Tham, Y., Tomé, A., Vazquez-Pufleau, M., Vogel, A., Wagner, R., Wang, M., Wang, D.,
1147   Wang, Y., Weber, S., Wu, Y., Xiao, M., Yan, C., Ye, P., Ye, Q., Zauner-Wieczorek, M., Zhou, X.,
1148   Baltensperger, U., Dommen, J., Flagan, R., Hansel, A., Kulmala, M., Volkamer, R., Winkler, P.,
1149   Worsnop, D., Donahue, N., Kirkby, J. and Curtius, J.: Molecular understanding of new-particle
1150   formation from alpha-pinene between &#8722;50&#8201;&#176;C and
1151   25&#8201;&#176;C, Atmos. Chem. Phys., (January), 1–42, doi:10.5194/acp-2019-1058,
1152   2020.

1153   Sindelarova, K., Granier, C., Bouarar, I., Guenther, A., Tilmes, S., Stavrakou, T., Müller, J. F., Kuhn, U.,
1154   Stefani, P. and Knorr, W.: Global data set of biogenic VOC emissions calculated by the MEGAN model
1155   over the last 30 years, Atmos. Chem. Phys., 14(17), 9317–9341, doi:10.5194/ACP-14-9317-2014,
1156   2014.

1157   Singh, B. P., Kumar, K. and Jain, V. K.: Source identification and health risk assessment associated
1158   with particulate- and gaseous-phase PAHs at residential sites in Delhi, India, Air Qual. Atmos. Heal.,
1159   doi:10.1007/S11869-021-01035-5, 2021.

1160   Singh, D. P., Gadi, R. and Mandal, T. K.: Characterization of Gaseous and Particulate Polycyclic
1161   Aromatic Hydrocarbons in Ambient Air of Delhi, India, Polycycl. Aromat. Compd., 32(4), 556–579,

1162   doi:10.1080/10406638.2012.683230, 2012.

1163   Sinha, V., Kumar, V. and Sarkar, C.: Chemical composition of pre-monsoon air in the Indo-Gangetic
1164   Plain measured using a new air quality facility and PTR-MS: High surface ozone and strong influence
1165   of biomass burning, Atmos. Chem. Phys., 14(12), 5921–5941, doi:10.5194/acp-14-5921-2014, 2014.

1166   Spolnik, G., Wach, P., Rudzinski, K. J., Skotak, K., Danikiewicz, W. and Szmigielski, R.: Improved
1167   UHPLC-MS/MS Methods for Analysis of Isoprene-Derived Organosulfates, Anal. Chem., 90(5), 3416–
1168   3423, doi:10.1021/acs.analchem.7b05060, 2018.

1169   Stewart, G. J., Nelson, B. S., Acton, W. J. F., Vaughan, A. R., Farren, N. J., Hopkins, J. R., Ward, M. W.,
1170   Swift, S. J., Arya, R., Mondal, A., Jangirh, R., Ahlawat, S., Yadav, L., Sharma, S. K., Yunus, S. S. M.,
1171   Hewitt, C. N., Nemitz, E., Mullinger, N., Gadi, R., Sahu, L. K., Tripathi, N., Rickard, A. R., Lee, J. D.,
1172   Mandal, T. K. and Hamilton, J. F.: Emissions of intermediate-volatility and semi-volatile organic
1173   compounds from domestic fuels used in Delhi, India, Atmos. Chem. Phys., 21(4), 2407–2426,
1174   doi:10.5194/ACP-21-2407-2021, 2021a.

1175   Stewart, G. J., Acton, W. J. F., Nelson, B. S., Vaughan, A. R., Hopkins, J. R., Arya, R., Mondal, A.,
1176   Jangirh, R., Ahlawat, S., Yadav, L., Sharma, S. K., Dunmore, R. E., Yunus, S. S. M., Nicholas Hewitt, C.,
1177   Nemitz, E., Mullinger, N., Gadi, R., Sahu, L. K., Tripathi, N., Rickard, A. R., Lee, J. D., Mandal, T. K. and
1178   Hamilton, J. F.: Emissions of non-methane volatile organic compounds from combustion of domestic
1179   fuels in Delhi, India, Atmos. Chem. Phys., 21(4), 2383–2406, doi:10.5194/ACP-21-2383-2021, 2021b.

1180   Stewart, G. J., Nelson, B. S., Drysdale, W. S., Acton, W. J. F., Vaughan, A. R., Hopkins, J. R., Dunmore,
1181   R. E., Hewitt, C. N., Nemitz, E., Mullinger, N., Langford, B., Shivani, Reyes-Villegas, E., Gadi, R.,
1182   Rickard, A. R., Lee, J. D. and Hamilton, J. F.: Sources of non-methane hydrocarbons in surface air in
1183   Delhi, India, Faraday Discuss., 226(0), 409–431, doi:10.1039/D0FD00087F, 2021c.

1184   Surratt, J. D., Murphy, S. M., Kroll, J. H., Ng, N. L., Hildebrandt, L., Sorooshian, A., Szmigielski, R.,
1185   Vermeylen, R., Maenhaut, W., Claeys, M., Flagan, R. C. and Seinfeld, J. H.: Chemical composition of
1186   secondary organic aerosol formed from the photooxidation of isoprene, J. Phys. Chem. A, 110(31),
1187   9665–9690, doi:10.1021/jp061734m, 2006.

1188   Surratt, J. D., Kroll, J. H., Kleindienst, T. E., Edney, E. O., Claeys, M., Sorooshian, A., Ng, N. L.,
1189   Offenberg, J. H., Lewandowski, M., Jaoui, M., Flagan, R. C. and Seinfeld, J. H.: Evidence for
1190   Organosulfates in Secondary Organic Aerosol, Environ. Sci. Technol., 41(2), 517–527,
1191   doi:10.1021/es062081q, 2007.

1192   Surratt, J. D., Gómez-González, Y., Chan, A. W. H., Vermeylen, R., Shahgholi, M., Kleindienst, T. E.,
1193   Edney, E. O., Offenberg, J. H., Lewandowski, M., Jaoui, M., Maenhaut, W., Claeys, M., Flagan, R. C.
1194   and Seinfeld, J. H.: Organosulfate Formation in Biogenic Secondary Organic Aerosol, J. Phys. Chem. A,
1195   112(36), 8345–8378, doi:10.1021/jp802310p, 2008a.

1196   Surratt, J. D., Gómez-González, Y., Chan, A. W. H., Vermeylen, R., Shahgholi, M., Kleindienst, T. E.,
1197   Edney, E. O., Offenberg, J. H., Lewandowski, M., Jaoui, M., Maenhaut, W., Claeys, M., Flagan, R. C.
1198   and Seinfeld, J. H.: Organosulfate Formation in Biogenic Secondary Organic Aerosol, J. Phys. Chem. A,
1199   112(36), 8345–8378, doi:10.1021/jp802310p, 2008b.

1200   Surratt, J. D., Chan, A. W. H., Eddingsaas, N. C., Chan, M., Loza, C. L., Kwan, A. J., Hersey, S. P., Flagan,
1201   R. C., Wennberg, P. O. and Seinfeld, J. H.: Reactive intermediates revealed in secondary organic
1202   aerosol formation from isoprene, Proc. Natl. Acad. Sci., 107(15), 6640–6645,
1203   doi:10.1073/pnas.0911114107, 2010.

1204   Szidat, S., Jenk, T. M., Gäggeler, H. W., Synal, H. A., Fisseha, R., Baltensperger, U., Kalberer, M.,
1205   Samburova, V., Wacker, L., Saurer, M., Schwikowski, M. and Hajdas, I.: Source apportionment of
1206   aerosols by 14C measurements in different carbonaceous particle fractions, in Radiocarbon, vol. 46,

1207   pp. 475–484, University of Arizona., 2004.

1208   Takeuchi, M. and Ng, N. L.: Chemical composition and hydrolysis of organic nitrate aerosol formed
1209   from hydroxyl and nitrate radical oxidation of α-pinene and β-pinene, Atmos. Chem. Phys., 19(19),
1210   12749–12766, doi:10.5194/ACP-19-12749-2019, 2019.

1211   Wagner, P. and Kuttler, W.: Biogenic and anthropogenic isoprene in the near-surface urban
1212   atmosphere — A case study in Essen, Germany, Sci. Total Environ., 475, 104–115,
1213   doi:10.1016/J.SCITOTENV.2013.12.026, 2014.

1214   Wang, J. L., Chew, C., Chang, C. Y., Liao, W. C., Lung, S. C. C., Chen, W. N., Lee, P. J., Lin, P. H. and
1215   Chang, C. C.: Biogenic isoprene in subtropical urban settings and implications for air quality, Atmos.
1216   Environ., 79, 369–379, doi:10.1016/J.ATMOSENV.2013.06.055, 2013.

1217   Wang, X. K., Rossignol, S., Ma, Y., Yao, L., Wang, M. Y., Chen, J. M., George, C. and Wang, L.:
1218   Molecular characterization of atmospheric particulate organosulfates in three megacities at the
1219   middle and lower reaches of the Yangtze River, Atmos. Chem. Phys., 16(4), 2285–2298,
1220   doi:10.5194/acp-16-2285-2016, 2016.

1221   Wang, Y., Hu, M., Guo, S., Wang, Y., Zheng, J., Yang, Y., Zhu, W., Tang, R., Li, X., Liu, Y., Le Breton, M.,
1222   Du, Z., Shang, D., Wu, Y., Wu, Z., Song, Y., Lou, S., Hallquist, M. and Yu, J.: The secondary formation
1223   of organosulfates under interactions between biogenic emissions and anthropogenic pollutants in
1224   summer in Beijing, Atmos. Chem. Phys., 18(14), 10693–10713, doi:10.5194/acp-18-10693-2018,
1225   2018a.

1226   Wang, Y., Hu, M., Guo, S., Wang, Y., Zheng, J., Yang, Y., Zhu, W., Tang, R., Li, X., Liu, Y., Le Breton, M.,
1227   Du, Z., Shang, D., Wu, Y., Wu, Z., Song, Y., Lou, S., Hallquist, M. and Yu, J.: The secondary formation
1228   of organosulfates under interactions between biogenic emissions and anthropogenic pollutants in
1229   summer in Beijing, Atmos. Chem. Phys., 18(14), 10693–10713, doi:10.5194/acp-18-10693-2018,
1230   2018b.

1231   Wang, Y., Tong, R. and Yu, J. Z.: Chemical Synthesis of Multifunctional Air Pollutants: Terpene-
1232   Derived Nitrooxy Organosulfates, Environ. Sci. Technol., acs.est.1c00348,
1233   doi:10.1021/acs.est.1c00348, 2021a.

1234   Wang, Y., Zhao, Y., Wang, Y., Yu, J. Z., Shao, J., Liu, P., Zhu, W., Cheng, Z., Li, Z., Yan, N. and Xiao, H.:
1235   Organosulfates in atmospheric aerosols in shanghai, china: Seasonal and interannual variability,
1236   origin, and formation mechanisms, Atmos. Chem. Phys., 21(4), 2959–2980, doi:10.5194/acp-21-
1237   2959-2021, 2021b.

1238   Wennberg, P. O., Bates, K. H., Crounse, J. D., Dodson, L. G., McVay, R. C., Mertens, L. A., Nguyen, T.
1239   B., Praske, E., Schwantes, R. H., Smarte, M. D., St Clair, J. M., Teng, A. P., Zhang, X. and Seinfeld, J. H.:
1240   Gas-Phase Reactions of Isoprene and Its Major Oxidation Products, Chem. Rev., 118(7), 3337–3390,
1241   doi:10.1021/acs.chemrev.7b00439, 2018.

1242   WHO: WHO | Ambient air pollution, WHO, 2018.

1243   Wozniak, A. S., Bauer, J. E. and Dickhut, R. M.: Characteristics of water-soluble organic carbon
1244   associated with aerosol particles in the eastern United States, Atmos. Environ., 46, 181–188,
1245   doi:10.1016/j.atmosenv.2011.10.001, 2012.

1246   Xu, J., Song, S., Harrison, R. M., Song, C., Wei, L., Zhang, Q., Sun, Y., Lei, L., Zhang, C., Yao, X., Chen,
1247   D., Li, W., Wu, M., Tian, H., Luo, L., Tong, S., Li, W., Wang, J., Shi, G., Huangfu, Y., Tian, Y., Ge, B., Su,
1248   S., Peng, C., Chen, Y., Yang, F., Mihajlidi-Zelić, A., Đordević, D., Swift, S. J., Andrews, I., Hamilton, J. F.,
1249   Sun, Y., Kramawijaya, A., Han, J., Saksakulkrai, S., Baldo, C., Hou, S., Zheng, F., Daellenbach, K. R.,
1250   Yan, C., Liu, Y., Kulmala, M., Fu, P. and Shi, Z.: An interlaboratory comparison of aerosol inorganic ion

1251 measurements by ion chromatography: Implications for aerosol pH estimate, Atmos. Meas. Tech.,
1252 13(11), 6325–6341, doi:10.5194/AMT-13-6325-2020, 2020.

1253 Xu, L., Guo, H., Boyd, C. M., Klein, M., Bougiatioti, A., Cerully, K. M., Hite, J. R., Isaacman-VanWertz,
1254 G., Kreisberg, N. M., Knote, C., Olson, K., Koss, A., Goldstein, A. H., Hering, S. V., Gouw, J. de,
1255 Baumann, K., Lee, S.-H., Nenes, A., Weber, R. J. and Ng, N. L.: Effects of anthropogenic emissions on
1256 aerosol formation from isoprene and monoterpenes in the southeastern United States, Proc. Natl.
1257 Acad. Sci., 112(1), 37–42, doi:10.1073/PNAS.1417609112, 2015.

1258 Yadav, A. K., Sarkar, S., Jyethi, D. S., Rawat, P., Aithani, D., Siddiqui, Z. and Khillare, P. S.: Fine
1259 Particulate Matter Bound Polycyclic Aromatic Hydrocarbons and Carbonaceous Species in Delhi's
1260 Atmosphere: Seasonal Variation, Sources, and Health Risk Assessment, Aerosol Sci. Eng. 2021 52,
1261 5(2), 193–213, doi:10.1007/S41810-021-00094-6, 2021.

1262 Yee, L. D., Isaacman-VanWertz, G., Wernis, R. A., Kreisberg, N. M., Glasius, M., Riva, M., Surratt, J. D.,
1263 de Sá, S. S., Martin, S. T., Alexander, M. L., Palm, B. B., Hu, W., Campuzano-Jost, P., Day, D. A.,
1264 Jimenez, J. L., Liu, Y., Misztal, P. K., Artaxo, P., Viegas, J., Manzi, A., de Souza, R. A. F., Edgerton, E. S.,
1265 Baumann, K. and Goldstein, A. H.: Natural and Anthropogenically Influenced Isoprene Oxidation in
1266 Southeastern United States and Central Amazon, Environ. Sci. Technol.,
1267 doi:10.1021/acs.est.0c00805, 2020.

1268 Zhang, H., Yee, L. D., Lee, B. H., Curtis, M. P., Worton, D. R., Isaacman-VanWertz, G., Offenberg, J. H.,
1269 Lewandowski, M., Kleindienst, T. E., Beaver, M. R., Holder, A. L., Lonneman, W. A., Docherty, K. S.,
1270 Jaoui, M., Pye, H. O. T., Hu, W., Day, D. A., Campuzano-Jost, P., Jimenez, J. L., Guo, H., Weber, R. J.,
1271 De Gouw, J., Koss, A. R., Edgerton, E. S., Brune, W., Mohr, C., Lopez-Hilfiker, F. D., Lutz, A., Kreisberg,
1272 N. M., Spielman, S. R., Hering, S. V., Wilson, K. R., Thornton, J. A. and Goldstein, A. H.: Monoterpenes
1273 are the largest source of summertime organic aerosol in the southeastern United States, Proc. Natl.
1274 Acad. Sci. U. S. A., 115(9), 2038–2043, doi:10.1073/pnas.1717513115, 2018.

1275 Zhang, H., Zhang, Y., Huang, Z., Acton, W. J. F., Wang, Z., Nemitz, E., Langford, B., Mullinger, N.,
1276 Davison, B., Shi, Z., Liu, D., Song, W., Yang, W., Zeng, J., Wu, Z., Fu, P., Zhang, Q. and Wang, X.:
1277 Vertical profiles of biogenic volatile organic compounds as observed online at a tower in Beijing, J.
1278 Environ. Sci., 95, 33–42, doi:10.1016/J.JES.2020.03.032, 2020.

1279 Zhao, D., Schmitt, S. H., Wang, M., Acir, I. H., Tillmann, R., Tan, Z., Novelli, A., Fuchs, H., Pullinen, I.,
1280 Wegener, R., Rohrer, F., Wildt, J., Kiendler-Scharr, A., Wahner, A. and Mentel, T. F.: Effects of NOx
1281 and SO2 on the secondary organic aerosol formation from photooxidation of α-pinene and
1282 limonene, Atmos. Chem. Phys., 18(3), 1611–1628, doi:10.5194/acp-18-1611-2018, 2018.

1283 Zhao, D. F., Kaminski, M., Schlag, P., Fuchs, H., Acir, I. H., Bohn, B., Häseler, R., Kiendler-Scharr, A.,
1284 Rohrer, F., Tillmann, R., Wang, M. J., Wegener, R., Wildt, J., Wahner, A. and Mentel, T. F.: Secondary
1285 organic aerosol formation from hydroxyl radical oxidation and ozonolysis of monoterpenes, Atmos.
1286 Chem. Phys., 15(2), 991–1012, doi:10.5194/ACP-15-991-2015, 2015.

1287 Zou, Y., Deng, X. J., Deng, T., Yin, C. Q. and Li, F.: One-year characterization and reactivity of isoprene
1288 and its impact on surface ozone formation at a suburban site in Guangzhou, China, Atmosphere
1289 (Basel)., 10(4), doi:10.3390/ATMOS10040201, 2019.

1290